

10-A892 994

AIRESEARCH CASTING CO TORRANCE CA  
INJECTION MOLDING OF SINTERABLE SILICON-BASE, NONOXIDE CERAMICS--ETC(U)  
DEC 78 D L MANN F33615-77-C-5064  
78-15537 NL

UNCLASSIFIED

AFML-TR-78-200

F/8 13/8

10-A892 994

1

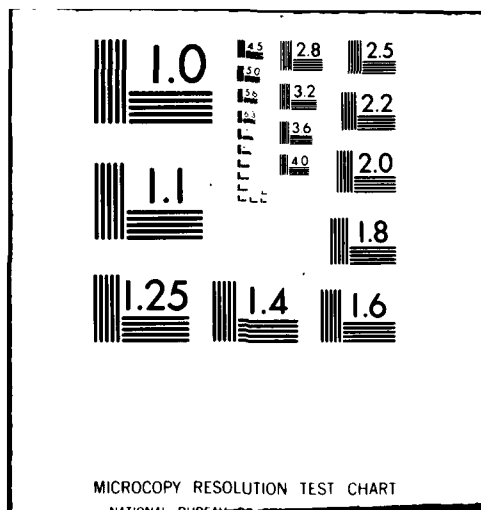
END

DATE

FILMED

-81

DTIC



AFML-TR-78-200

LEVEL II

①

AD A092994

## INJECTION MOLDING OF SINTERABLE SILICON-BASE, NONOXIDE CERAMICS

David L. Mann

AiResearch Casting Company  
2525 W. 190th Street  
Torrance, California 90509

December 1978

Technical Report AFML-TR-78-200  
Final Report for Period 1 September 1977 - 31 October 1978

DTIC  
ELECTE  
DEC 16 1980  
S E

Approved for public release: distribution unlimited.

Air Force Materials Laboratory  
Air Force Wright Aeronautical Laboratories  
Air Force Systems Command  
Wright-Patterson Air Force Base, Ohio 45433

FILE COPY

80 12 15 043

## NOTICE


When Government drawings, specifications, or other data are used for any purpose other than in connection with a definitely related Government procurement operation, the United States Government thereby incurs no responsibility nor any obligation whatsoever; and the fact that the government may have formulated, furnished, or in any way supplied the said drawings, specifications, or other data, is not to be regarded by implication or otherwise as in any manner licensing the holder or any other person or corporation, or conveying any rights or permission to manufacture, use, or sell any patented invention that may in any way be related thereto.

This report has been reviewed by the Information Office (OI) and is releasable to the National Technical Information Service (NTIS). At NTIS, it will be available to the general public, including foreign nations.

This technical report has been reviewed and is approved for publication.

  
K.S. MAZDIYASNI  
Project Engineer

FOR THE COMMANDER

  
JEROME K. ELBAUM  
ACTING CHIEF  
Processing and High Temperature Materials Branch  
Metals and Ceramics Division

If your address has changed, if you wish to be removed from our mailing list, or if the addressee is no longer employed by your organization please notify AFMD/LLM, W-PAFB, OH 45433 to help us maintain a current mailing list.

Copies of this report should not be returned unless return is required by security considerations, contractual obligations, or notice on a specific document.

UNCLASSIFIED

SECURITY CLASSIFICATION OF THIS PAGE (When Data Entered)

REPORT DOCUMENTATION PAGE		READ INSTRUCTIONS BEFORE COMPLETING FORM
1. RESEARCH NUMBER AFML-TR-78-200	2. GOVT ACCESSION NO. AD-A092 994	3. RECIPIENT'S CATALOG NUMBER
4. TITLE (and Subtitle) INJECTION MOLDING OF SINTERABLE SILICON-BASE, NONOXIDE CERAMICS.	5. TYPE OF REPORT & REMOD COVERED Final Report. 1 Sep 1977-31 Oct 1978	6. PERFORMING ORG. REPORT NUMBER 78-15537
7. AUTHOR(s) David L. Mann	8. CONTRACT OR GRANT NUMBER(s) F33615-77-C-5064	9. PROGRAM ELEMENT, PROJECT, TASK AREA & WORK UNIT NUMBERS ILIR 00-90
9. PERFORMING ORGANIZATION NAME AND ADDRESS AirResearch Casting Company 2525 W. 190th St. Torrance, Calif. 90509	10. REPORT DATE December 1978	11. NUMBER OF PAGES 74
11. CONTROLLING OFFICE NAME AND ADDRESS Air Force Materials Laboratory (LLM) Wright-Patterson AF Base, OH 45433	12. SECURITY CLASS. (of this report) Unclassified	13. DECLASSIFICATION/DOWNGRADING SCHEDULE
14. MONITORING AGENCY NAME & ADDRESS (if different from Controlling Office) 1285	15. DISTRIBUTION STATEMENT (of this Report) Approved for public release; distribution unlimited.	
17. DISTRIBUTION STATEMENT (of the abstract entered in Block 20, if different from Report)		
18. SUPPLEMENTARY NOTES		
19. KEY WORDS (Continue on reverse side if necessary and identify by block number) Silicon nitride Injection molding Sintering Binder		
20. ABSTRACT (Continue on reverse side if necessary and identify by block number) The program has resulted in a process for fabricating complex shapes of sinterable, silicon-based, nonoxide ceramic by injection molding a materials system consisting of submicron silicon nitride powder, sintering aids, and organic lubricant/binder. It is felt that this process also is capable of accommodating alternate sinterable materials and sintering aids.		

DD FORM 1 JAN 73 1473 EDITION OF 1 NOV 65 IS OBSOLETE

UNCLASSIFIED  
SECURITY CLASSIFICATION OF THIS PAGE (When Data Entered)

412 048

45

UNCLASSIFIED

SECURITY CLASSIFICATION OF THIS PAGE(When Data Entered)

➤ GTE Sylvania SN502 grade silicon nitride was chosen as the primary candidate material for the injection molding investigation. At the start of the program, SN502 best met the program prerequisites of commercial availability in large quantities and previously demonstrated sinterability. This material was used with yttrium oxide additions to develop a baseline injection molding composition from which processing and compositional variations could be made. A previously developed organic lubricant/binder system and binder extraction technique were used.

↖ It was found that the SN502 powder milled with silicon nitride media would not sinter to acceptable densities with the use of yttrium oxide alone. Therefore, controlled additions of aluminum oxide were made and a composition of 88 weight/percent silicon nitride, 8 weight/percent yttrium oxide, and 4 weight/percent aluminum oxide sintered to 3.2 gm/cc fairly readily. An alternative to this system proposed by GTE was to use a Sylvania powder (3512) that already contained proprietary sintering aids. This material was evaluated, but it did not have the sinterability necessary to meet program requirements. The SN502-based system therefore was carried on for the final process development effort and AFML specimen fabrication.

UNCLASSIFIED

SECURITY CLASSIFICATION OF THIS PAGE(When Data Entered)

## PREFACE

The research work described in this final report was performed under Contract No. F33615-77-C-5064. Mr. K. S. Mazdidasni of the Air Force Materials Laboratory, Wright-Patterson AFB, was the project engineer. Mr. Karsten H. Styhr was the AirResearch Casting Company program manager, and Mr. David L. Mann was the principal investigator.

The author would like to express his appreciation to Ishver K. Naik for his contributions and many discussions regarding materials phase equilibria, to Floyd G. Larson for assistance in the X-Ray diffraction analysis and interpretation, and to Steven Haynes and Lonnie Anderson for their skillful efforts in the processing activities of the program.

Accession For	
NTIS GRA&I	<input checked="checked" type="checkbox"/>
DDC TAB	<input type="checkbox"/>
Unannounced Justification	<input type="checkbox"/>
By _____	
Distribution/	
Availability Codes	
Dist.	Avail and/or special
A	

## SUMMARY

The program has resulted in a process for fabricating complex shapes of sinterable, silicon-based, nonoxide ceramic by injection molding a materials system consisting of submicron  $\text{Si}_3\text{N}_4$  powder, sintering aids, and organic lubricant/binder. It is felt that this process also is capable of accommodating alternate sinterable materials and sintering aids.

As a result of reviewing silicon-based ceramic technology and available silicon-based powders ( $\text{Si}_3\text{N}_4$  and  $\text{SiC}$ ), GTE Sylvania SN502 grade silicon nitride was chosen as the primary candidate material for the injection molding investigation. SN502 best met the program prerequisites of commercial availability in large quantities and previously demonstrated sinterability. This material was used with  $\text{Y}_2\text{O}_3$  additions to develop a baseline injection molding composition from which processing and compositional variations could be made. A previously developed organic lubricant/binder system and binder extraction technique were used. The early baseline composition sintered to high (>95 percent of theoretical) density; however,  $\text{Al}_2\text{O}_3$  grinding media were used and significant  $\text{Al}_2\text{O}_3$  contents were noticed by XRD of milled powders.

To preclude uncontrolled introduction of any material that might influence the system behavior (e.g.,  $\text{Al}_2\text{O}_3$ ),  $\text{Si}_3\text{N}_4$  media were used. It was found that the 502 powder milled with  $\text{Si}_3\text{N}_4$  media would not sinter to acceptable densities with the use of  $\text{Y}_2\text{O}_3$  alone. Therefore, controlled additions of  $\text{Al}_2\text{O}_3$  were made and a composition of 88  $\text{Si}_3\text{N}_4$ , 8  $\text{Y}_2\text{O}_3$ , and 4  $\text{Al}_2\text{O}_3$  sintered to 3.2 gm/cc fairly readily. Although not yet proven, reference to the phase diagrams for this system indicated that the resultant second phase would be glassy and therefore might produce less than optimum high-temperature mechanical properties. An alternative to this system proposed by GTE was to use a Sylvania powder (3512) that already contained proprietary sintering aids. This material was evaluated, but it did not have the sinterability necessary to meet program requirements. The 502-based system, therefore, was carried on for the final process development effort and AFML specimen fabrication. Further investigation of the 3512 powder at GTE Waltham laboratories, WESGO, and GTE Towanda resulted in the conclusion that this lot of powder would not sinter as previous batches of 3512 had done at GTE. As a consequence of this situation, GTE is investigating their powder processing with the goal of increasing reproducibility.

## TABLE OF CONTENTS

<u>Section</u>	<u>Page</u>
I INTRODUCTION	1
1.1 Scope	1
1.2 Objectives	1
1.3 Prerequisites	1
II BACKGROUND	2
2.1 GTE Sylvania	3
2.2 Stanford Research Institute	3
2.3 Army Materials and Mechanics Research Center	4
2.4 General Electric Corporate Research Laboratory	4
2.5 Additional Technical Review	4
III EXPERIMENTAL PROGRAM	7
3.1 Materials Selection	9
3.2 Materials Characterization	10
3.3 Injection Batch Preparation	21
3.4 Injection Molding	35
3.5 Binder Extraction	41
3.6 Sintering	41
3.7 Properties Measurement	66
3.8 Process Description	71
IV CONCLUSIONS	72
V RECOMMENDATIONS	73
REFERENCES	74

## LIST OF ILLUSTRATIONS

<u>Figure</u>		<u>Page</u>
1	Injection Molding Schematic	8
2	Si <sub>3</sub> N <sub>4</sub> 502, Lot 04-12, X-Ray Diffraction Pattern	11
3	Si <sub>3</sub> N <sub>4</sub> 502, Lot 04-46, X-Ray Diffraction Pattern	12
4	GTE Sylvania Lot 04-46, Type SN502 Silicon Nitride Powder	13
5	GTE Sylvania Lot 04-12, Type SN502 Silicon Nitride Powder	14
6	Particle Size Distribution Measurements	15
7	Molycorp Yttrium Oxide Type 5600, Lot 803	16
8	Particle Size Distribution Curve	17
9	Linde-A Al <sub>2</sub> O <sub>3</sub> , Lot 418	18
10	Effect of Dry Ball Milling Time on SN502 Si <sub>3</sub> N <sub>4</sub> Powder Appearance	23
11	Effect of Dry Ball Milling Time on SN502 Si <sub>3</sub> N <sub>4</sub> Powder Appearance	24
12	X-Ray Radiograph Demonstrating Flaws in Injection Run No. 12127xx	28
13	X-Ray Radiograph Showing Injection-Molded Stator Vanes Using Batch 116-25	29
14	As-Injected Stator Vane and Test Bars	30
15	Test Bar Tool in Position in Arburg Injection Machine	32
16	Cold Pressed Green Density vs Milling Time	35
17	Injection Molding Die T-62042-1 Installed in Injection Molding Machine	36
18	Injection Molding Die T-62044	37
19	Parts Produced with Die T-62044 in Typical Molding Operation	38
20	Results of Injection Molding Experiment Using Spiral Flow Mold Tooling	40

# LIST OF ILLUSTRATIONS (Continued)

<u>Figure</u>		<u>Page</u>
21	Results of Proper and Improper Binder Extraction	42
22	Dewaxed Vanes from Batch 116-25 (70 percent solids) Ready to Sinter	42
23	Vacuum/Pressure Furnace and Motor Generator Set	43
24	Sintered $\text{Si}_3\text{N}_4$ + 4 Weight/Percent $\text{Y}_2\text{O}_3$ , 1923°K, 1 hr	44
25	Sintered Stator Vanes	45
26	Dry-Pressed Discs Sintered Inside and Outside of $\text{Si}_3\text{N}_4$ Sagger	46
27	X-Ray Diffraction Pattern of As-Received GTE 502 $\text{Si}_3\text{N}_4$ Powder	47
28	X-Ray Diffraction Pattern of GTE 502 $\text{Si}_3\text{N}_4$ Powder with 4 Weight/Percent $\text{Y}_2\text{O}_3$ Added	49
29	X-Ray Diffraction Pattern of Material from Figure 27 after Sintering	50
30	Sintered Density vs Weight/Percent of $\text{Al}_2\text{O}_3$	52
31	Sintered Density vs Sintering Time at 2023°K	52
32	Microstructure of $\text{Si}_3\text{N}_4$ Specimens	54
33	Polished Sections of 16-43 Material	55
34	X-Ray Diffraction Pattern of As-Sintered MOR Specimen	47
35	X-Ray Diffraction Pattern of MOR Specimen after 2400°K Test in Air	58
36	Weight Loss vs Time at 2023°K for Injection Molded Specimens	59
37	Sintered Density vs Sintering Time at 2023°K	61
38	Scanning Electron Micrographs of 88 wt/% $\text{Si}_3\text{N}_4$ , 8 wt/% $\text{Y}_2\text{O}_3$ , 4 wt/% $\text{Al}_2\text{O}_3$ Sintered at Various Temperatures and Times	63

LIST OF ILLUSTRATIONS (Continued)

<u>Figure</u>		<u>Page</u>
39	Scanning Electron Micrographs Showing Increased Surface Porosity with Sintering Time	67
40	4-Point Flexural Strength Fixture	68
41	Large Defect on Tensile Surface of Sintered MOR Specimen	60
42	Apparent Fracture Origin in 61 KSI MOR Test Specimen	70

## LIST OF TABLES

<u>Table</u>		<u>Page</u>
1	Chemical Analysis Results, GTE Sylvania SN502 Silicon Nitride, Lots 04-12 and 04-46	19
2	Chemical Analyses of Molycorp 5600 Yttrium Oxide and Union Carbide Linde-A Aluminum Oxide	20
3	Powder Preparation	22
4	Silicon Nitride Injection Molding Batches	25
5	Injection Molding Parameters and Results	26
6	Silicon Nitride Injection Molding Batches	27
7	Injection Details for Vans and Stator Bars	30
8	Optimum Machine Settings for Test Bar Injection	31
9	Ball-Milling Effect on Green Density of Cold-Pressed Discs	33
10	Pressing Pressure vs Density for Ball-Milled and Cold-Pressed 3512 $\text{Si}_3\text{N}_4$	33
11	Components for 700-gm Batch of Composition 16-43	34
12	Injection Molding Parameters	39
13	Sintering Run Parameters	45
14	Sintering Study Summary	51
15	Preliminary Modulus of Rupture (MOR) Measurements	53
16	1273°K Weight Loss Summary	56
17	Sintering Response of Composition 3512 to Powder Preparation	60
18	Sintering Parameter Study	62
19	Modulus of Rupture Results	68
20	Test Specimen Process and Materials	71

## SECTION I

### INTRODUCTION

#### 1.1 SCOPE

This program comprised research and exploratory development of the process of injection-molding sinterable, silicon-base, nonoxide ceramics.

#### 1.2 OBJECTIVES

One objective of the program was to develop a practical, low-cost technique for the fabrication of complex, precision, sinterable, silicon-based nonoxide ceramic components for such applications as small, limited-life RPV and APU turbine engines, rocket and laser nozzles, or radomes, using injection molding. A second objective was to make available test specimens suitable for physical and thermomechanical property measurements by the AFML or its designee.

#### 1.3 PREREQUISITES

Prerequisites for candidate raw materials were that they would be commercially available in reasonably large quantities and that they would have been previously demonstrated to be sinterable to greater than 95 percent of theoretical density. Therefore, the effort included a screening and selection of such raw materials as silicon carbides, silicon nitrides, and other materials suitable for injection or transfer molding of complex, precision ceramic shapes.

## SECTION II

### BACKGROUND

High performance turbine engines demand that turbine components maintain their structural integrity and strength at extremes of temperature and environmental stress. Advances in turbine engine design technology in many respects have become material-limited as the operating temperatures have increased. Considerable research in this area has recently focused on using ceramics for the highest temperature components. Ceramics offer a great potential for higher operating temperatures and thus, greater system efficiencies. Some estimates are that operating temperatures as high as 1623°K may be realized when ceramics are incorporated into small turbine engines. These engines have the potential for increased efficiencies, lower exhaust emissions, improved specific fuel consumption, as well as higher power per unit weight. There also is an incentive to replace superalloys, which are costly and of limited supply, with more abundant ceramics that also will have a much lower material cost. The use of ceramics is also favored by such additional considerations as their low bulk density, excellent erosion/corrosion/oxidation resistance, long-range availability, and potentially lower cost. Ceramics, however, with their low resistance to tensile stresses and lack of ductility require brittle-material design approaches. They also require improved quality assurance techniques. The design engineer must be able to apply stress analysis techniques that will closely approximate the service conditions.

Equally important as these design constraints is the ability of the ceramic component manufacturer to repeatedly produce reliable, homogeneous, reproducible components that not only meet the dimensional specifications of the design, but also consistently meet or exceed the materials performance specifications of any particular application. While the properties of ceramics in turbine service environments are now beginning to be determined and understood by the design engineer, the producibility of structural ceramics remains a pacing problem.

Hot-pressed SiC and Si<sub>3</sub>N<sub>4</sub> are superior in room temperature strength to the sintered products of either system. Presently, however, hot pressing is shape limited and requires substantial diamond grinding and/or ultrasonic machining to form a finished complex shape. Because high volume ceramic manufacturing operations must avoid finish grinding whenever possible to meet cost goals, the performance superiority of hot pressing may well be offset by the lower-cost potential of a near-net-shape sintering process.

Process development for ceramics based on ionic compounds has been continuous over the last two decades and is well known throughout the ceramic industry. The same is not true, however, for ceramics based on predominantly covalently bonded compounds such as Si<sub>3</sub>N<sub>4</sub> and SiC. Densification of these materials has

been achieved only by the liberal use of sintering or hot pressing aids. Unfortunately, the presence of these aids in most cases has led to degradation of the desired high temperature properties and stability of the material.

An initial review of laboratories concerned with sinterable, silicon-based nonoxide ceramics, or organizations that would be potential suppliers of raw material to produce such products, was completed during the first quarter of the program (October through December 1977). Conclusions from this survey follow.

## 2.1 GTE SYLVANIA

At the time of the survey, two types of silicon-nitride powder were commercially available from GTE Sylvania: (1) an amorphous-type, code SN402, and (2) a crystalline-type, code SN502. Neither type contains a sintering aid and neither may be sintered to greater than 95 percent of theoretical density as purchased. It has been demonstrated in the Sylvania Laboratory that both types can be further processed and compounded with sintering aids and ultimately sintered to above 95 percent density. Sylvania is not prepared to discuss details of their "further processing" at this time; however, they referred us to several research laboratories who independently made similar demonstrations of sinterability.

Sylvania personnel recommended that the primary candidate for injection molding purposes should be the SN502, a 60-percent crystalline, alpha-phase  $\text{Si}_3\text{N}_4$ . The sintering aid with the greatest technical data base is yttrium oxide ( $\text{Y}_2\text{O}_3$ ). The amount of this additive, alternate additives, homogenizing conditions, and sintering schedules were discussed with GTE personnel. Such preconditioning of powders for injection molding as prepressing and granulating, using alkoxy-derived  $\text{Y}_2\text{O}_3$  for the sintering aid, spray drying or calcining, were discussed as possible processing steps. It was mentioned that a third form of Sylvania  $\text{Si}_3\text{N}_4$  powder might become available as a commercial material in the future. It would be a preconditioned product containing a homogeneous sintering aid ready for a forming process. This turned out to be the SN3512 material tested later in the program.

## 2.2 STANFORD RESEARCH INSTITUTE

Stanford Research Institute (SRI) has been investigating the sintering of GTE Sylvania powders and alternate powders under NSF sponsorship for about two years. They have had the most success with Sylvania SN402 powder, having achieved over 99 percent of theoretical density using  $\text{Y}_2\text{O}_3$ , a very high isostatic pressing pressure of 690 MPa (100,000 psi) and sintering at 1923°K (1650°C) for 5 hr at 1 atmosphere positive nitrogen pressure. A review of mixing, milling, pressing, handling, and sintering conditions by SRI personnel is gratefully acknowledged.

### 2.3 ARMY MATERIALS AND MECHANICS RESEARCH CENTER

Army Materials and Mechanics Research Center (AMMRC) personnel have been investigating various sintering aid additions to several  $\text{Si}_3\text{N}_4$  powders including Sylvania products. Additives include  $\text{CeO}_2$ ,  $\text{Y}_2\text{O}_3$ ,  $\text{MgAl}_2\text{O}_4$ ,  $\text{Y}_2\text{Al}_2\text{O}_6$ ,  $\text{Be}_3\text{N}_2$ , and others. The most positive results to date are with  $\text{Y}_2\text{O}_3$ , with the amount of added  $\text{Y}_2\text{O}_3$  based on the oxygen content of the starting  $\text{Si}_3\text{N}_4$  powder. Initial experiments based on 4 percent by weight  $\text{Y}_2\text{O}_3$  with additional  $\text{Y}_2\text{O}_3$  incorporated to react with the available oxygen to form an equimolar  $\text{Y}_2\text{O}_3 \cdot \text{SiO}_2$  compound, appear most desirable.

Preliminary experiments at AMMRC directed at injection molding silicon nitride powders using polyolefin binder systems were reviewed with AMMRC personnel. Very significant powder loadings have been achieved and some as-molded test pieces appeared very good. All attempts at binder removal had resulted in blistering, and no attempts at sintering molded shapes had been made at the date of review.

### 2.4 GENERAL ELECTRIC CORPORATE RESEARCH LABORATORY

General Electric Corporate Research Laboratory (GE CRL) has been investigating densification of both silicon carbides and silicon nitrides by hot pressing and sintering for a number of years. Current efforts include research toward improved high temperature properties of sintered  $\text{Si}_3\text{N}_4$  by the use of such nonoxide sintering aids as  $\text{BeSiN}_2$ . This work was reported to be in an early developmental stage, and current equipment to reach the high pressures and high temperatures that now appear necessary severely limit sample size and number of specimens per sintering cycle. GE personnel concurred that  $\text{Y}_2\text{O}_3$  additions to Sylvania powders appeared most suitable for developing the injection molding process.

### 2.5 ADDITIONAL TECHNICAL REVIEW

Discussions also were held with other investigators active in such related silicon ceramic systems as pressureless sintering, hot pressing of silicon nitride, and the complex family of materials generally referred to as "Sialons". These discussions were based upon the most current analytical and crystallographic understanding available, which required an awareness of current literature. A brief summary of the more pertinent discussions follows.

AiResearch Casting Company participated in a silicon nitride analytical symposium at Kawecky Berylco, Inc. and in a round-robin analytical investigation that resulted in the development at AiResearch of quantitative X-ray diffraction techniques. D. Messier of AMMRC, who was instrumental in the pioneering work in that area, shared details of his basic investigation of quantitative X-ray diffraction of  $\text{Si}_3\text{N}_4$  in a visit.

Phase relationships in the Si-Y-Al-N-O system and the associated technical literature on sintering were discussed with Dr. I.K. Naik\* of the University of Michigan (Ref. 1). It has become apparent from these discussions and from the literature that a system containing no oxides other than  $Y_2O_3$  cannot be sintered at the temperatures of interest. Although the primary component of the liquid phase at sintering temperature is  $SiO_2$ , some  $Al_2O_3$  and/or  $Y_2O_3$  must be present for the liquid phase to form. Discussions on sintering in the  $Si_3N_4$ - $Y_2O_3$  system were also held with Dr. D.J. Rowcliffe of SRI. Rowcliffe and Jorgensen have shown that no densification occurs in sintering experiments even with 4-percent  $Y_2O_3$  present when the  $Si_3N_4$  powder used (GTE 402) has been previously deoxidized by vacuum annealing in the presence of 1-percent carbon (Ref. 2).

The bulk of Rowcliffe's work has involved the sintering of cold-pressed  $Si_3N_4$  powder compacts (GTE SN402) containing from 4 to 17 weight/percent  $Y_2O_3$ . His material also contained 2.7 weight/percent oxygen (by neutron activation analysis), probably as  $SiO_2$  and significant amounts of  $Al_2O_3$  picked up unintentionally during milling. Sintered density was shown to be relatively independent of  $Y_2O_3$  content within the range investigated; however, the role of  $Al_2O_3$  picked up unintentionally during milling was not clarified. At low  $Y_2O_3$  levels (4 to 8 weight/percent), there was large scatter in the densification behavior for short sintering times (1 to 2 hr). This was possibly due to varying amounts of  $Al_2O_3$  introduced during milling.

It is generally accepted that sintering occurs by dissolution of  $Si_3N_4$  in the liquid phase, transport along particle boundaries, and continuous reprecipitation. The process apparently always leads to the hexagonal beta- $Si_3N_4$  structure, or to the beta solid solution with the same structure and slightly larger lattice parameters. The stoichiometry of the beta solid solution is stated to be  $Si_{6-x}Al_xO_xN_{8-x}$ ; that is, it lies along the join between  $Si_3N_4$  and  $(Al_2O_3 \cdot AlN)$ . Jack (Ref. 3) has published data on the effect of dissolved aluminum and oxygen on beta lattice parameters.

Rowcliffe's current work also suggests that in  $Si_3N_4$ , which contains  $Y_2O_3$  and  $Al_2O_3$ , the latter is partitioned between the liquid and the crystalline phases during sintering. That is, the  $Al_2O_3$  first dissolves in the liquid phase, but as sintering proceeds, a portion of it dissolves in the solid, or  $Si_3N_4$  (beta to beta prime), phase. The above is deduced from the fact that more  $Al_2O_3$  is found in the beta solid solution (lattice parameters are larger) when  $Y_2O_3$  content is low (less liquid phase) than when  $Y_2O_3$  content is high (more liquid phase). Although beta lattice parameters may be influenced by the presence of  $Y_2O_3$  in solid solution, the effect would be expected to be the opposite of that observed. The practical implication of this phenomenon is that removal of  $Al_2O_3$  from the liquid phase during sintering would be expected to change its properties. The "softening" temperature would probably increase and devitrification might be influenced. Such changes could be expected to improve high-temperature properties.

---

\*Since that time, Dr. Naik has joined the AiResearch Casting Company.

Because the survey of contemporary work emphasized the importance of intentionally and milling-added impurities to sintering behavior, special attention was given to the levels of such compositions as  $Y_2O_3$ ,  $Al_2O_3$ ,  $SiO_2$  (or oxygen), etc., and their effect on final product density. A great deal of this information was obtained from the contemporary work of other investigators. References are made to phase diagrams and literature on the  $Y_2O_3$ - $SiO_2$ - $Al_2O_3$  system (Refs. 4, 5, 6).

### SECTION III

#### EXPERIMENTAL PROGRAM

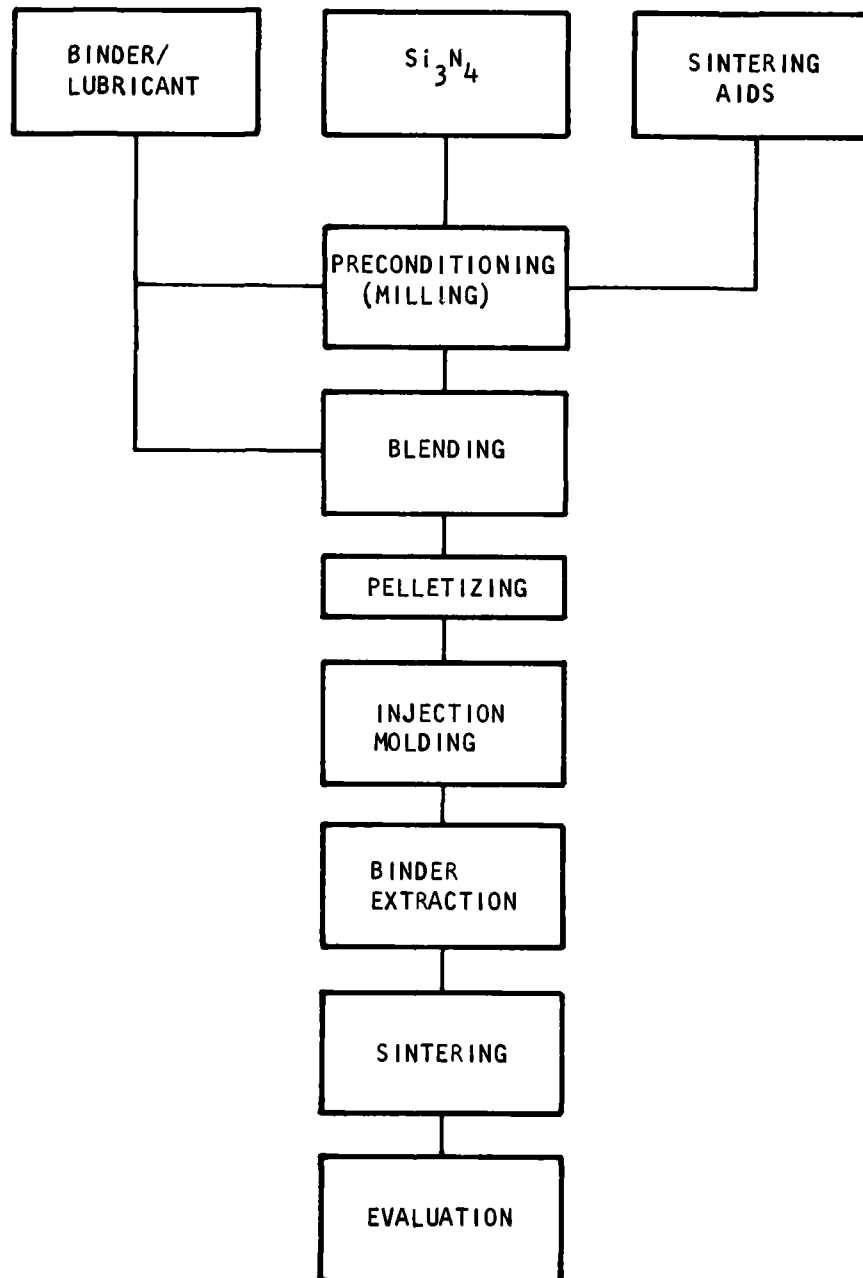
Development of techniques for the fabrication of sinterable silicon-based, nonoxide ceramics using injection molding necessitated the early establishment of a baseline composition capable of being molded into specimens suitable for evaluation. Consequently, a primary candidate  $\text{Si}_3\text{N}_4$  material (GTE Sylvania SN502) was selected for early mix development. An organic lubricant/binder system previously developed at AiResearch Casting Company (ACC) also was selected and with these materials, many injectable mixes were made and used to determine the effect of such parameters as powder preconditioning; binder composition and loading; injection pressure; holding pressure; temperatures of the material, nozzle, and mold; and cavity fill rate. A schematic of the injection molding process is shown in Figure 1. Alternate starting powders and compositional variations were investigated after establishment of the injectable baseline mix and the injection molding process itself was better defined for these materials.

After demonstrating the ability to successfully fabricate a complex shape, the effects on end properties (primarily sintered density), of variables such as milling media, green density, sintering aids, and sintering cycles were evaluated. It was found that the SN502 would not sinter to the desired density (95 percent  $\gamma$ ) with the use of the recommended  $\text{Y}_2\text{O}_3$  alone, but that batches milled with  $\text{Al}_2\text{O}_3$  media would. Attempts were made to optimize a system containing both  $\text{Al}_2\text{O}_3$  and  $\text{Y}_2\text{O}_3$ . Another possible candidate starting powder designated as SN3512 was obtained from GTE Sylvania. This material contained GTE Sylvania proprietary sintering aids already mixed with silicon nitride and, per recommendation of GTE Sylvania, would supposedly sinter to high density using AiResearch sintering conditions and thus yield good mechanical properties.

The two starting powders, viz., (1) SN502 with 8 weight/percent  $\text{Y}_2\text{O}_3$  and 4 weight/percent  $\text{Al}_2\text{O}_3$  and (2) SN3512, were evaluated and compared during Task 1B. On the basis of sintered density, the SN502 with 8 weight/percent  $\text{Y}_2\text{O}_3$  and 4 weight/percent  $\text{Al}_2\text{O}_3$  as sintering aids, was selected for the remainder of the work. A previously developed paraffin-based organic system, LN27-266-2,\* was used for the injection binder/lubricant.

While it was felt that this material best fitted the primary objective of developing an injection molding fabrication technique (by sintering to high densities, phenomena such as the effect of full shrinkage on part distortion could be evaluated), it was recognized that the  $\text{Y}_2\text{O}_3$  and  $\text{Al}_2\text{O}_3$ , with the 2 to 3 weight/percent oxygen present in the  $\text{Si}_3\text{N}_4$  powder, would probably result in a glassy boundary phase with less than desirable high temperature creep and flexural strengths. However, it was beyond the scope of this effort to pursue the sintering aid optimization.

\*J.F. McCaughin Co., Rosemead, Ca.



S-24999 A

Figure 1. Injection Molding Process Schematic

### 3.1 MATERIALS SELECTION

#### 3.1.1 Starting Materials

An initial technical review of laboratories concerned with sinterable, silicon-based nonoxide ceramics, or organizations that are potential suppliers of raw material to produce such products, was completed during the first quarter of the program. Sylvania SN502 and SN402 powders best met the program prerequisites, and both were obtained. Other materials for use in this program as sintering aids, such as HTM  $Y_2O_3$ ,\* Molycorp  $Y_2O_3$ ,\*\* and Linde-A  $Al_2O_3$ ,\*\*\* were obtained. HTM  $Y_2O_3$  is an alkoxy-derived ultra-high-purity material that was developed specifically to provide the ultra-small particle size most suitable for producing a homogeneous body when incorporated as a sintering aid. Molycorp  $Y_2O_3$  also is a high-purity (99.99 percent pure) material with approximately 15 ppm Ca as the main impurity and average particle size of 2  $\mu m$ . Linde-A  $Al_2O_3$  is a high-purity, submicron particle size material that is compatible with the other batch components.

The following alternate sources were investigated:

Carborundum Company--Sinterable alpha silicon carbide powder was not commercially available from Carborundum for use on this program.

Kawecki Berylco Industries-- $Si_3N_4$  powders potentially suitable for sintering now are made domestically, at least in small quantities. Commercial history and previous demonstration of sintering to 95 percent of theoretical density was not sufficiently documented to consider their use on this program.

PPG Industries--Sinterable beta silicon carbide powders were not commercially available from PPG, although internal development work was reported to be continuing.

H. C. Stark Co.--A sample of silicon nitride powder was purchased for evaluation; however, sinterability to 95 percent of theoretical density was not sufficiently documented to consider this a primary candidate material for use on this program.

Sonneborn Refractories and Chemicals--3000 lb of a feed material for producing high purity, fine particle size, beta-phase silicon carbide powders was reported to be available. No demonstration of sinterability has been reported; therefore, it was not a primary candidate material for use in this program.

Excelon Corporation--Excelon imports large quantities of alpha-phase silicon carbide grain. A substantial portion of this can be processed into a fine, particle-size powder, which with suitable sintering additives, potentially could be further processed into a sinterable powder. No demonstration of such sinterability has yet been reported.

\*HTM Company, Cincinnati, Ohio.

\*\*Molycorp, York, Pa.

\*\*\*Linde Division of Union Carbide.

Kyocera International--Several silicon nitride powders of various alpha-to-beta phase ratios were available commercially. No demonstration of sinterability was available from the supplier.

HTM Company--This company specializes in reactive powder preparations such as those derived from alkoxides. Attempts at their processing Sylvania powders to incorporate  $Y_2O_3$  sintering aid directly and homogeneously did not appear practical. They supplied a fine-particle size (2500 Å)  $Y_2O_3$  for use by AiResearch.

### 3.2 MATERIALS CHARACTERIZATION

X-ray diffraction patterns for the two lots of SN502 silicon nitride powders are shown in Figures 2 and 3. A Norelco diffractometer with  $CuK\alpha$  radiation was used with a scan rate of 2 deg/min. The two lots were GTE Sylvania lot numbers 04-112 and 04-46. The results for both lots show that of the crystalline phase present, approximately 95 percent is alpha phase and approximately 5 percent is beta phase. There is a noticeable difference at 28.6 deg  $2\theta$ , which indicates that lot 04-46 has free silicon while the 04-112 material does not. More detailed analyses are discussed in para. 3.6.2.

Scanning electron micrographs (SEM) of the two lots (Figures 4 and 5) show similar mixtures of acicular crystals and clusters of submicron spheres. Spheroid diameters ranging from 0.25 to 0.75  $\mu m$  were observed in the sample viewed. The alpha phase needles on the other hand are typically less than 1  $\mu m$  in diameter with an L/D of up to 100  $\mu m$ .

Prior to the SEM observations, particle size distribution measurements were attempted using a Micromeritics\* X-Ray sedigraph. The measured resultant average spherical diameter was 2.5  $\mu m$  (as shown in Figure 6). The size distribution ranged from 0.2  $\mu m$  to approximately 40  $\mu m$ . While this might be a valid value of the equivalent spherical diameter, it obviously is not a true representation of the actual material as shown by the SEM photographs.

The Molycorp  $Y_2O_3$  used in the experimental batches consists of irregular, angular particles that have an average size of 4.2  $\mu m$ . SEM photos of the material are shown in Figure 7. The particle size distribution curve is shown in Figure 8.

The Linde-A alumina is a well-characterized, commercial, submicron-size, high-purity material. Typical particle size and morphology is shown in Figure 9.

The surface area of each of the materials was measured using a Micromeritics 2200 nitrogen absorption instrument. The two  $Si_3N_4$  powders were essentially the same: lot 04-12 had a surface area of 4.3  $m^2/gm$  and 04-46 had 4.4  $m^2/gm$ . The yttrium oxide has an area of 9.5  $m^2/gm$  and the alumina has 13.4  $m^2/gm$ .

Chemical analyses of each of the materials were run by Coors Spectro Chemical Laboratories, Golden, Colorado. The results are given in Tables 1 and 2.

\*Micromeritics Instruments Corporation, Norcross, Georgia.

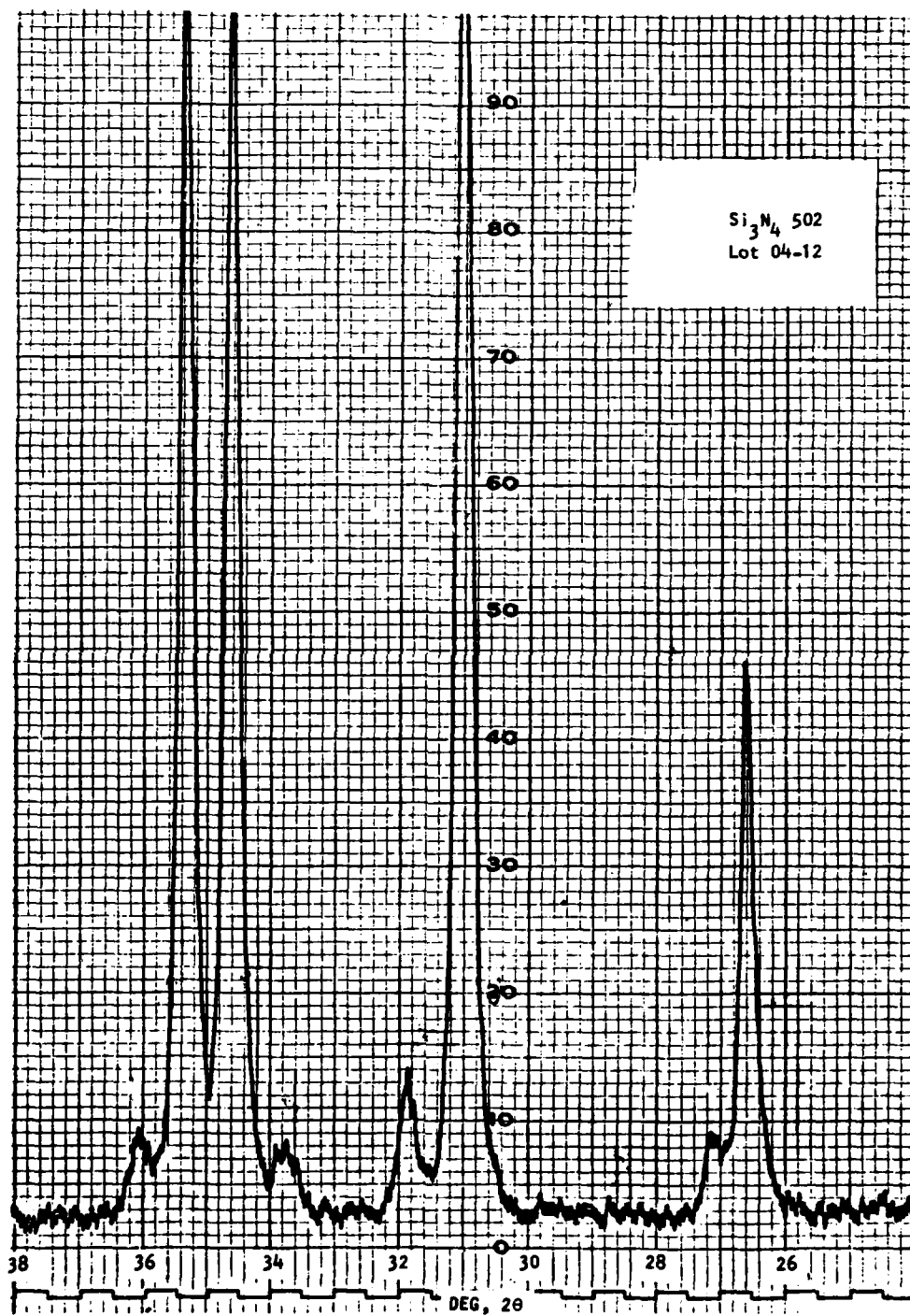


Figure 2. Si<sub>3</sub>N<sub>4</sub> 502, Lot 04-12, X-Ray Diffraction Pattern

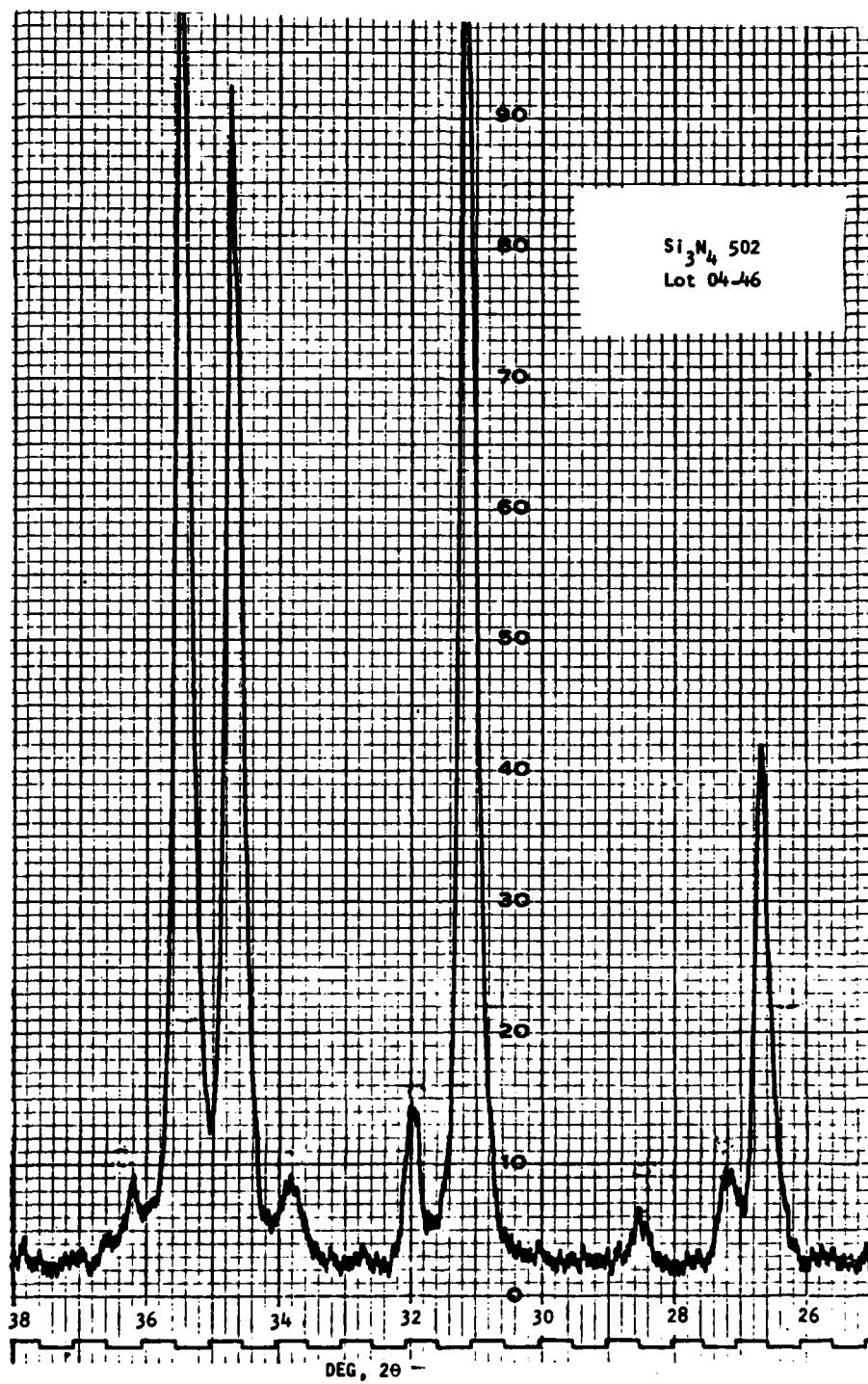


Figure 3. Si<sub>3</sub>N<sub>4</sub> 502, Lot 04-46, X-Ray Diffraction Pattern

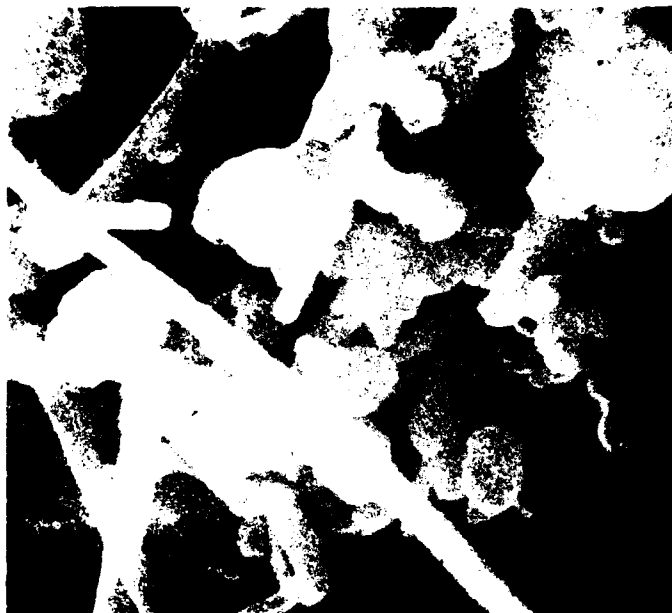


10 μm

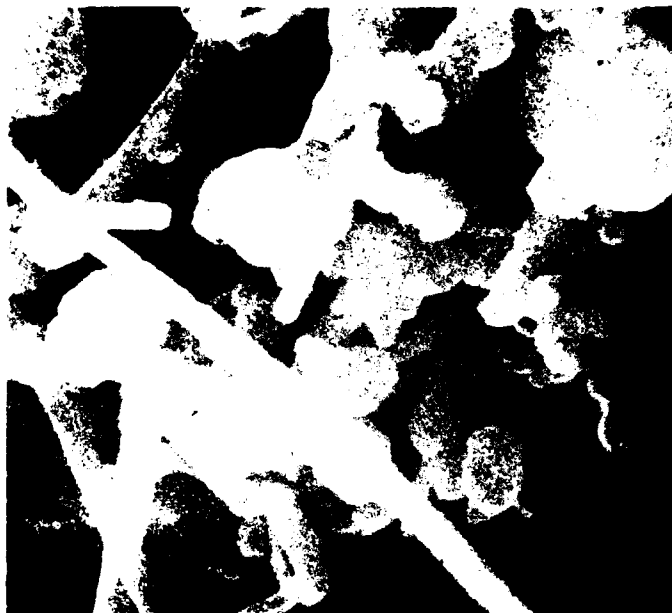


1 μm

Figure 4. GTE Sylvania Lot 04-46, Type SN502 Silicon Nitride Powder



10 μm



1 μm

Figure 5. GTE Sylvania Lot 04-12, Type SN502 Silicon Nitride Powder

# PARTICLE SIZE DISTRIBUTION

SAMPLE IDENTIFICATION 04-12 Si<sub>3</sub>N<sub>4</sub> 502  
 DATE 10/17/78  
 Density 3.2 g/cc LIQUID H<sub>2</sub>O Density g/cc Viscosity cp  
 BY R. C. CLOUD  
 TEMPERATURE 32°C  
 RATE 173 START DIA. 50 μm  
 Preparation

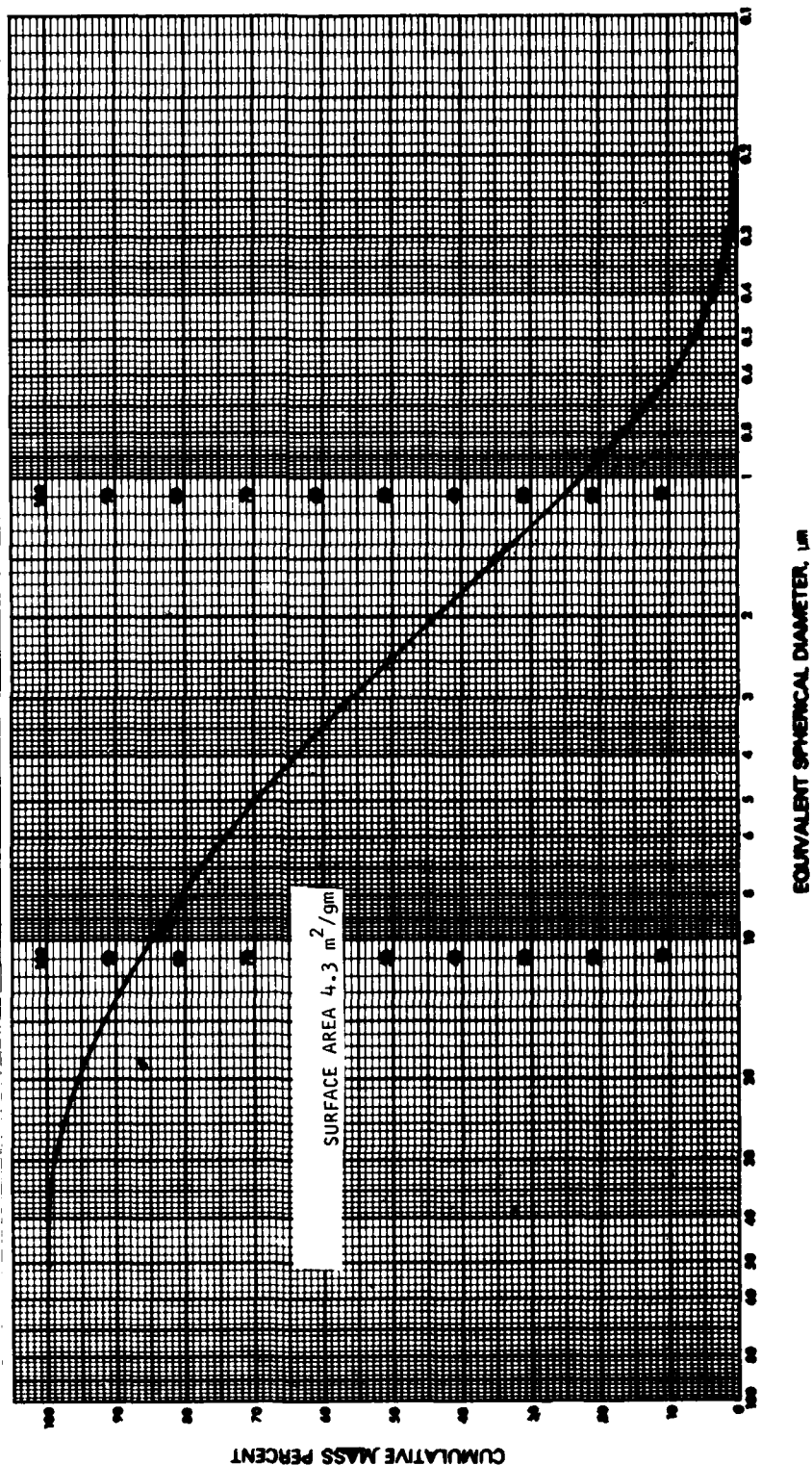


Figure 6. Particle Size Distribution Measurements

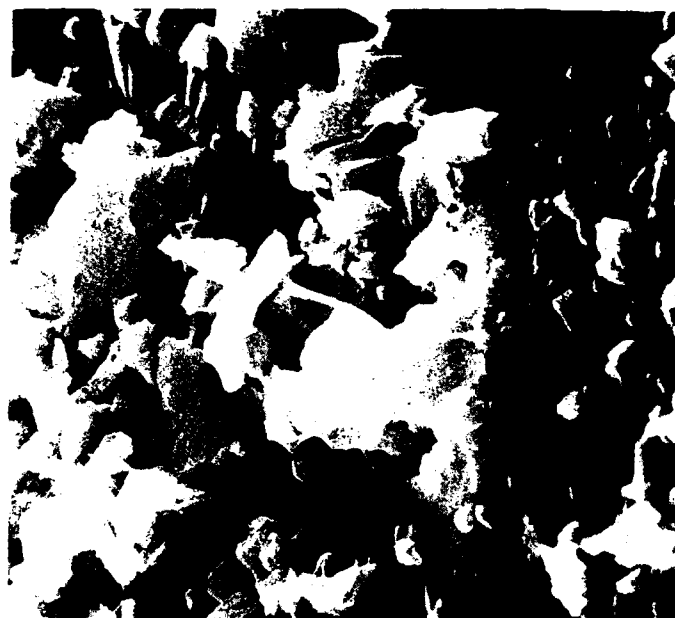


Figure 7. Molycorp Yttrium Oxide Type 5600, Lot 803

# PARTICLE SIZE DISTRIBUTION

SAMPLE IDENTIFICATION Y<sub>2</sub>O<sub>3</sub> 78-0244 DATE 10/12/78  
 Density 5.01 g/cc LIQUID SiO<sub>2</sub> Density g/cc Viscosity cp BY R.C. CLOUD  
 Preparation TEMPERATURE 32 °C  
 RATE 218 START DIA. 50  $\mu\text{m}$

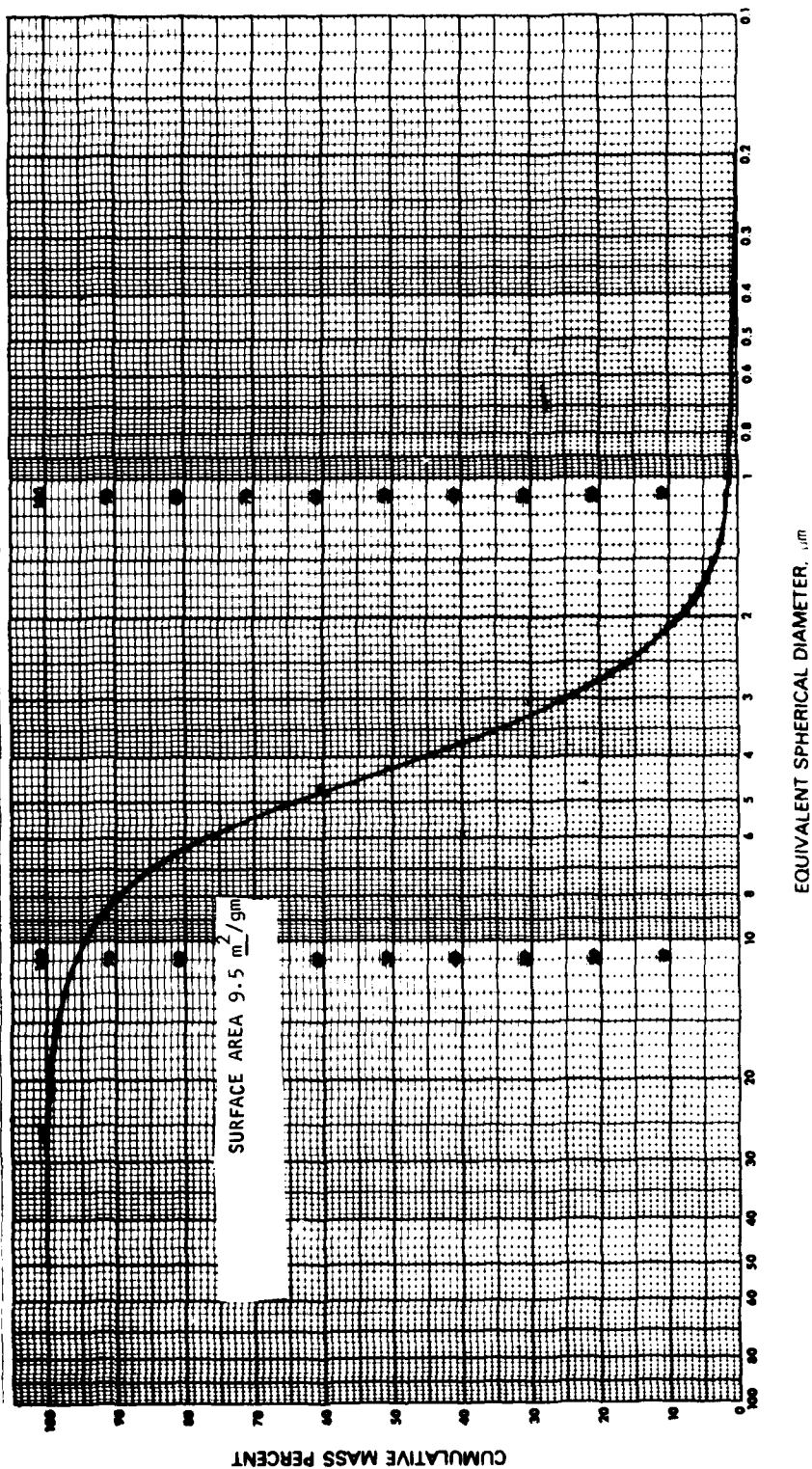


Figure 8. Particle Size Distribution Curve



1  $\mu\text{m}$

Figure 9. Linde-A  $\text{Al}_2\text{O}_3$ , Lot 418

TABLE 1  
CHEMICAL ANALYSIS RESULTS, GTE SYLVANIA SN502  
SILICON NITRIDE, LOTS 04-12 AND 04-46

$\text{Si}_3\text{N}_4$  Lot 04-46

ELEMENT	%	ELEMENT	%	ELEMENT	%	ELEMENT	%
Aluminum (Al)	0.01	Gallium (Ga)	< 0.005	Silicon (Si)	> 10	Rubidium (Rb)	
Antimony (Sb)	< 0.003	Germanium (Ge)	< 0.005	Silver (Ag)	< 0.001		
Arsenic (As)	< 0.01	Indium (In)	< 0.005	Strontium (Sr)	< 0.08		
Barium (Ba)		Iron (Fe)	0.008	Tin (Sn)	< 0.003		
Beryllium (Be)	< 0.001	Lead (Pb)	< 0.01	Titanium (Ti)	< 0.001		
Bismuth (Bi)	< 0.005	Magnesium (Mg)	0.005	Vanadium (V)	< 0.005		
Boron (B)	< 0.003	Manganese (Mn)	< 0.001	Zinc (Zn)	< 0.08		
Cadmium (Cd)	< 0.05	Mercury (Hg)		Zirconium (Zr)	< 0.01		
Calcium (Ca)	< 0.03	Molybdenum (Mo)	0.05	Sodium (Na)	< 0.05		
Chromium (Cr)	< 0.003	Nickel (Ni)	< 0.01	Cesium (Cs)			
Cobalt (Co)	< 0.01	Niobium (Nb)		Lithium (Li)	< 0.1		
Copper (Cu)	< 0.001	Phosphorus (P)	< 0.3	Potassium (K)			

$\text{Si}_3\text{N}_4$  Lot 04-12

ELEMENT	%	ELEMENT	%	ELEMENT	%	ELEMENT	%
Aluminum (Al)	0.01	Gallium (Ga)	< 0.005	Silicon (Si)	> 10	Rubidium (Rb)	
Antimony (Sb)	< 0.003	Germanium (Ge)	< 0.005	Silver (Ag)	< 0.001		
Arsenic (As)	< 0.01	Indium (In)	< 0.005	Strontium (Sr)	< 0.08		
Barium (Ba)		Iron (Fe)	0.01	Tin (Sn)	< 0.003		
Beryllium (Be)	< 0.001	Lead (Pb)	< 0.008	Titanium (Ti)	< 0.001		
Bismuth (Bi)	< 0.005	Magnesium (Mg)	0.005	Vanadium (V)	< 0.005		
Boron (B)	< 0.003	Manganese (Mn)	< 0.001	Zinc (Zn)	< 0.08		
Cadmium (Cd)	< 0.05	Mercury (Hg)		Zirconium (Zr)	< 0.01		
Calcium (Ca)	< 0.03	Molybdenum (Mo)	0.05	Sodium (Na)	< 0.05		
Chromium (Cr)	< 0.003	Nickel (Ni)	< 0.01	Cesium (Cs)			
Cobalt (Co)	< 0.01	Niobium (Nb)		Lithium (Li)	< 0.1		
Copper (Cu)	< 0.001	Phosphorus (P)	< 0.3	Potassium (K)			

TABLE 2  
CHEMICAL ANALYSES OF MOLYCORP 5600 YTTRIUM OXIDE  
AND UNION CARBIDE LINDE-A ALUMINUM OXIDE

Type 5600 Y<sub>2</sub>O<sub>3</sub>

ELEMENT	%	ELEMENT	%	ELEMENT	%	ELEMENT	%
Aluminum (Al)	< 0.01	Gallium (Ga)	< 0.005	Silicon (Si)	0.01	Rubidium (Rb)	
Antimony (Sb)	< 0.003	Germanium (Ge)	< 0.005	Silver (Ag)	0.004		
Arsenic (As)	< 0.01	Indium (In)	< 0.005	Strontium (Sr)	< 0.08		
Barium (Ba)		Iron (Fe)	0.02	Tin (Sn)	< 0.003		
Beryllium (Be)	< 0.001	Lead (Pb)	< 0.008	Titanium (Ti)	< 0.001		
Bismuth (Bi)	< 0.005	Magnesium (Mg)	0.005	Vanadium (V)	< 0.005		
Boron (B)	< 0.003	Manganese (Mn)	< 0.001	Zinc (Zn)	< 0.08		
Cadmium (Cd)	< 0.05	Mercury (Hg)		Zirconium (Zr)	< 0.01		
Calcium (Ca)	< 0.03	Molybdenum (Mo)	< 0.01	Sodium (Na)	< 0.05		
Chromium (Cr)	< 0.003	Nickel (Ni)	< 0.01	Cesium (Cs)			
Cobalt (Co)	< 0.01	Niobium (Nb)		Lithium (Li)	< 0.1		
Copper (Cu)	< 0.001	Phosphorus (P)	< 0.3	Potassium (K)			

Linde A Al<sub>2</sub>O<sub>3</sub>

ELEMENT	%	ELEMENT	%	ELEMENT	%	ELEMENT	%
Aluminum (Al)	> 10	Gallium (Ga)	< 0.005	Silicon (Si)	0.02	Rubidium (Rb)	
Antimony (Sb)	< 0.003	Germanium (Ge)	< 0.005	Silver (Ag)	< 0.001		
Arsenic (As)	< 0.01	Indium (In)	< 0.005	Strontium (Sr)	< 0.08		
Barium (Ba)		Iron (Fe)	0.007	Tin (Sn)	< 0.003		
Beryllium (Be)	< 0.001	Lead (Pb)	< 0.008	Titanium (Ti)	< 0.001		
Bismuth (Bi)	< 0.005	Magnesium (Mg)	0.003	Vanadium (V)	< 0.005		
Boron (B)	< 0.003	Manganese (Mn)	< 0.001	Zinc (Zn)	< 0.08		
Cadmium (Cd)	< 0.05	Mercury (Hg)		Zirconium (Zr)	< 0.01		
Calcium (Ca)	< 0.03	Molybdenum (Mo)	< 0.01	Sodium (Na)	< 0.05		
Chromium (Cr)	< 0.003	Nickel (Ni)	< 0.01	Cesium (Cs)			
Cobalt (Co)	< 0.01	Niobium (Nb)		Lithium (Li)	< 0.1		
Copper (Cu)	< 0.001	Phosphorus (P)	< 0.3	Potassium (K)			

### 3.3 INJECTION BATCH PREPARATION

The key to the injection molding of sound parts is the mix rheology--its flow behavior at the temperatures, pressures, and velocities required for complete compaction in the mold. Two process steps are involved in the batch preparation: (1) powder comminution and (2) powder/organic blending.

Ball milling was used to grind the powders to the size and shape that would give the desired flow characteristics at reasonably high ratios of powder-to-binder. Blending of the sintering aids with the  $\text{Si}_3\text{N}_4$  also was accomplished during the milling operation. The primary organic-powder blending was accomplished in a heated sigma blade mixer and completed during the screw plasticizing step of the injection cycle. Part quality and material flow requirements dictate that an intimate, homogeneous mix is obtained prior to injection.

#### 3.3.1 Powder Preparation

The powder contribution to the nature of the mix rheology is dependent on not only the volume fraction of solids, but also on the particle size, size-distribution, and shape. The as-manufactured powders typically are of a size and shape not conducive to injection molding; therefore, some type of preprocessing usually is required.

Dry milling, which has been successful in the preparation of injectable silicon batches, resulted in powder packing in the mill almost immediately, which effectively ended any significant comminution.

Rather than resorting to dry milling aids such as oleic acid, stearates, etc., which might have a deleterious effect on subsequent sintering, wet ball milling was chosen. Three wet-milled batches were prepared as shown in Table 3. Only the two batches milled in hexane appeared to mill properly and produce powders deemed acceptable for further processing. Two jar mill batches of each were prepared for injection molding.

Green density of cold-pressed discs was used as one measure of the effectiveness of the powder milling. Samples of the as-milled powders were formed in disc-shaped compacts (29-mm diameter by approximately 5 mm high) by uniaxial cold pressing in a steel die at 103 MPa. The parts were weighed, measured, and the bulk density was calculated.

The bulk densities of the wet-milled powders were lower than desired so different methods of dry ball milling were evaluated to increase milling effectiveness as well as to lessen the possibility of material segregation during evaporation of a milling solvent. It was found that the addition of 2 weight/percent stearic acid effectively prevented the powder from packing in the mill. Alumina milling media was first used, then steel, and finally  $\text{Si}_3\text{N}_4$  media.

Milling of  $\text{Si}_3\text{N}_4$  in a mill containing steel grinding media was more effective than milling with alumina media. Difficulty with the  $\text{Al}_2\text{O}_3$  media both in wet and dry milling was experienced due to the fluffy nature of the starting powder. This was not a problem with the steel media. It was found that powder milled with higher density steel media also produced higher green density, and exhibited better capability of being molded at a higher  $\text{Si}_3\text{N}_4$ -to-binder loading.

TABLE 3  
POWDER PREPARATION

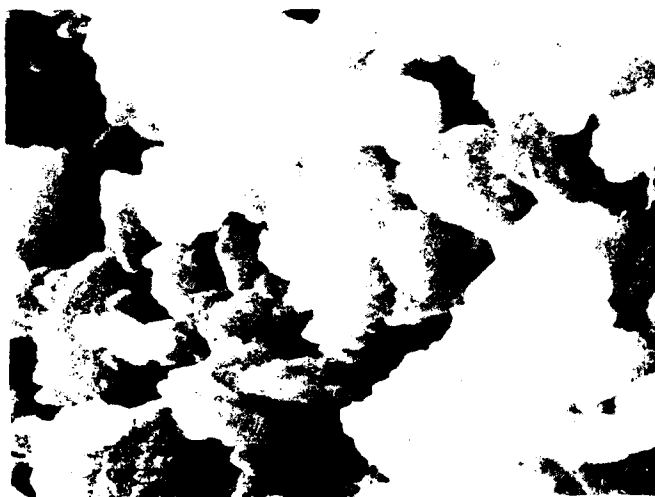
Experiment	Composition	Liquid	Mill time, hr	Green Density, gm/cc
1	100% $\text{Si}_3\text{N}_4$	None	0 (Caked)	-
2	100% $\text{Si}_3\text{N}_4$	Tert-Butyl Alcohol	4	1.39
3	100% $\text{Si}_3\text{N}_4$	Hexane	18	1.57
4	$\text{Si}_3\text{N}_4 + 4 \text{ Y}_2\text{O}_3$	Hexane	16	1.88
Mill Data: Mill-- $\text{Al}_2\text{O}_3$ 5-liter capacity jar Media--5-kg Coors $\text{Al}_2\text{O}_3$ 13/16 rod Mill speed--84 rpm Mill charge--400 gm powder: 1000 ml liquid				

All density determinations except for batch 116-25 were obtained from pressed discs. The fired density ( $\rho_f$ ) of the steel-milled batches was low (2.0 to 2.3 gm/cc). This may be due to either the lack of alumina or the presence of iron contamination. Alumina was added to a steel milled batch and fired density did increase slightly; however, due to the adoption of  $\text{Si}_3\text{N}_4$  media, this was not pursued.

The early efforts in batch preparation involved the study of parameters affecting the injection molding behavior rather than a concern for sintered properties. It was recognized that batch milling, either in alumina mill jars with alumina grinding media or in rubber-lined mills with steel or alumina grinding media, introduces substances that must be considered as contaminants or impurities. These impurities when added in uncontrolled quantities would not be conducive to reproducibility even if they were not detrimental to the final sintered part. Iron contamination could be removed by acid leaching; however, acid could produce changes in the  $\text{Si}_3\text{N}_4$  chemistry, such as oxidation, thus creating or adding a surface layer of  $\text{SiO}_2$  and altering both microstructure and stoichiometry. Therefore, the decision was reached not to attempt acid leaching, but rather, to obtain  $\text{Si}_3\text{N}_4$  grinding media, which was used for the balance of the investigations.

Scanning electron microscopy (SEM) and particle size determination were used to determine the effect of milling time on powder comminution and to ensure adequate reduction of the SN502 "needles". The SEM results of samples taken from mill batch 72\* at 4, 8, 16, and 24 hr are shown in Figures 10 and 11.

\*The batch composition was 616 gm SN502, 56 gm  $\text{Y}_2\text{O}_3$ , 28 gm  $\text{Al}_2\text{O}_3$  and 14 gm of stearic acid. This powder was milled with 2.2 kg of  $\text{Si}_3\text{N}_4$  media in a 20-cm ID, rubber-lined mill turning at 62.5 rpm.



24 HR



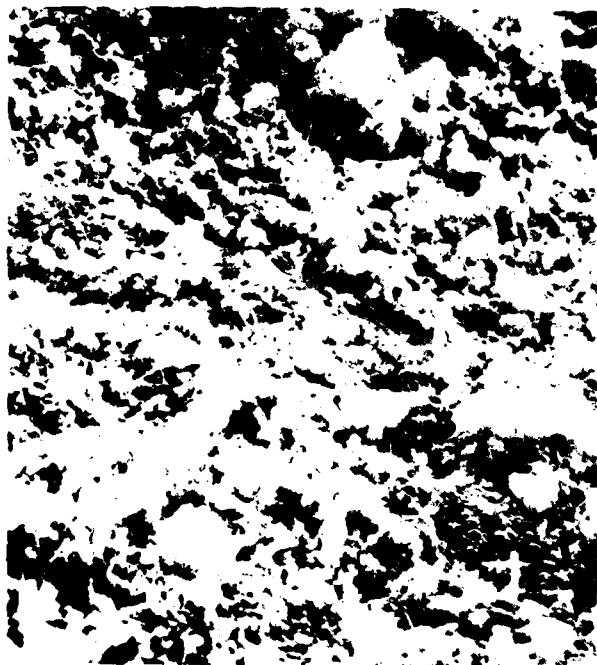
16 HR

1  $\mu m$



4 HR

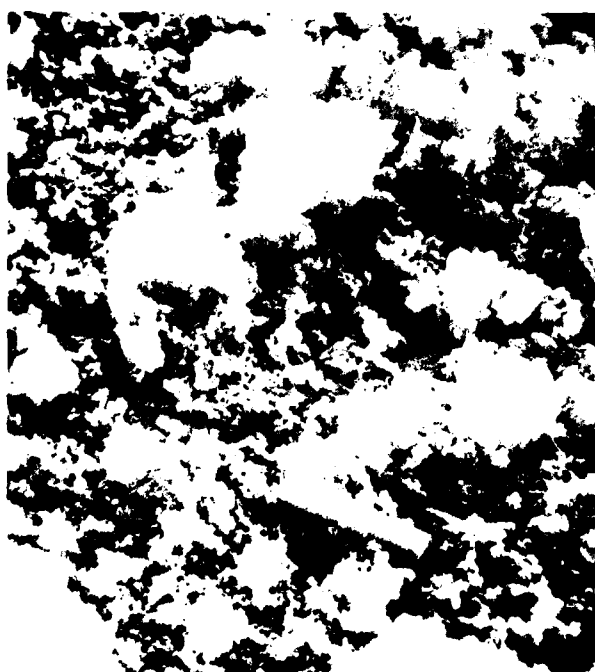
Figure 10. Effect of Dry Ball Milling Time on SN502  $Si_3N_4$  Powder Appearance



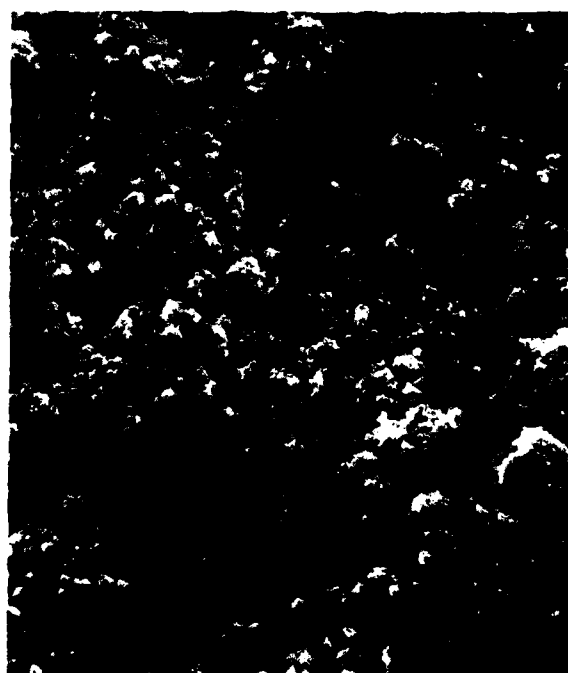
4 HR



8 HR



16 HR



24 HR

10  $\mu\text{m}$



Figure 11. Effect of Dry Ball Milling Time on SN502  $\text{Si}_3\text{N}_4$  Powder Appearance

The acicular crystals are very apparent at 4 hr. After 8 hr, considerable reduction had occurred, but some needle-like material was still present. The 16-hr samples showed essentially complete comminution of the material and no acicular particles were found in the 24-hr milled sample. The large, rod-shaped particle shown in the 16-hr material (Figure 11) was atypical; however, its presence is important since its anomalous size and shape probably would cause a low strength or defect region.

### 3.3.2 Injection Mix

Concurrent with the efforts to optimize the physical characteristics of the inorganic powders, studies were conducted on the inorganic/organic blend. The two most critical aspects of the injection mix preparation are the volume loading of solids and the homogeneity of the final mix. The volume loading is probably the most important variable controlling the final mix rheology. Loading levels between 54 and 74 volume/percent solids were evaluated. The batch summaries are given in Tables 4 and 5. It was found that a solids loading of 62.5 volume percent produced a very usable injection mix with the  $\text{Si}_3\text{N}_4$  media-milled powder. Equivalent ease of injection was possible at 66 volume/percent using steel-milled powder.

TABLE 4  
SILICON NITRIDE INJECTION MOLDING BATCHES

Batch No.	Green Density, gm/cc	Fired Density,* gm/cc	Milling Time, hr	Milling Media	Milling Environ.	Volume Percent $\text{Si}_3\text{N}_4$	Weight/Percent $\text{Y}_2\text{O}_3$	Weight/Percent Stearic Acid
116-2	1.54	3.03	16.3	$\text{Al}_2\text{O}_3$	Hexane	54.0	4	0
116-5	2.00	2.93	75.0	$\text{Al}_2\text{O}_3$	Hexane	59.0	4	0
116-14	1.20	1.97	8.0	$\text{Al}_2\text{O}_3$	4.5 hr Hexane; 3.5 hr dry	62.0	4	1.
116-20	1.90	2.00	5.0	Steel	Dry	71.0	4	2.
116-21	2.00	None fired	16.0	Steel	Dry	62.0	4	2.
116-25	2.02	2.33	16.0	Steel	Dry	70.0	4	2.

\*Fired densities were obtained on cold-pressed samples except 116-25, which was injection molded.

TABLE 5  
INJECTION MOLDING PARAMETERS AND RESULTS

Inj. Run	Configuration	Batch No.	Feed Zone Temp., °K	Plastic Zone Temp., °K	Nozzle Zone Temp., °K	Inj. Speed	Inj. Time, sec	Inj. Pressure, MPa	Mold Clamp Time, sec	Shot Length, cc	Mold Temp., °K	Results
1207701	Spiral	116-2	350	355	350	Max.	5	124	36	5.5	295	Flow 6 in.
1207702	Spiral	116-2	350	355	350	Max.	5	124	36	5.5	295	Flow 9 in.
1207703	Spiral	116-2	350	355	350	Max.	5	124	36	5.5	295	Flow 11 in.
1212701	Vane & test	116-2	350	355	350	Max.	5	124	36	4.0	300	Shrinkage flaws
1212703	Vane & test	116-2	350	355	350	Max.	5	117	36	4.0	300	Shrinkage flaws
1212704	Vane & test	116-2	350	355	350	Max.	5	110	36	4.0	300	Shrinkage flaws
1213704	Vane & test	116-2	344	350	339	Max.	5	110	36	3.5	300	Cracks in tab radii
01198xx	Vane & test	116-14	344	350	339	Max.	5	110	36	4.5	300	Very poor flow
01198xx	Vane & test	116-5	344	350	339	Max.	5	110	36	4.5	300	Very poor fill
02038xx	Vane & test	116-20	344	350	339	Max.	5	124	36	4.5	300	Partial mold fill
0213801	Vane & test	116-21	339	339	339	Max.	5	110	36	5	300	Mold flashed, good part
0213802	Vane & test	116-21	327	327	327	Max.	5	110	36	5	300	Decreased flash, good part
0220801	Vane & test	116-25	339	339	339	Max.	5	110	36	5	300	Excellent surface, good part

Table 4 summarizes the injection batches tested. Dry milling with steel media was found to yield a powder capable of being injected at relatively high solid content. Table 5 presents the results of the injection experiments using these mixes.

Early experiments revealed molding defects that varied in degree of severity with variations of injection molding parameters. Batch 116-2, run number 12127xx, contained porosity that variations in molding parameters (temperature, pressure, time, and speed) would not eliminate completely. Figure 12 is an X-ray radiograph demonstrating these flaws. Batch 116-14 had higher  $\text{Si}_3\text{N}_4$  to binder loading and, regardless of changes in molding parameters, resulted in incomplete mold filling and/or binding of the plasticizing screw.

The iterations described resulted in batch 116-25; steel milling media; 70 volume/percent solids;  $\text{Si}_3\text{N}_4$  + 4 weight/percent  $\text{Y}_2\text{O}_3$ . Despite the high solid-to-binder loading, this batch injection molded readily and produced excellent surface finish. This behavior is presumed to be due to the particle size distribution attained with the steel media. Figure 13 is an X-ray radiograph showing injection-molded stator vanes using batch 116-25. Figure 14 is a photograph of as-injected stator vane and test bars.

The next series of injection experiments were based on compositions found to yield the highest sinterability (i.e., 88 weight/percent  $\text{Si}_3\text{N}_4$  + 8 weight/percent  $\text{Y}_2\text{O}_3$  + 4 weight/percent  $\text{Al}_2\text{O}_3$ ). The injection mix data is summarized in Table 6.

TABLE 6  
SILICON NITRIDE INJECTION MOLDING BATCHES

Batch No.	Green Density, gm/cc	Fired Density, gm/cc	Milling Time, hr	Milling Media	Volume Percent $\text{Si}_3\text{N}_4$ plus Oxides	Comments
16-43	1.94	3.2+	24	$\text{Si}_3\text{N}_4$	62.5	GTE3512  No stearic acid
16-44	2.07	3.2+	16	Steel	66	
16-58	2.04	3.3+	24	$\text{Si}_3\text{N}_4$	62.5	
16-60	2.20	2.45	-	-	63.7	
16-68	1.83	3.2+	24	$\text{Si}_3\text{N}_4$	62.5	
16-72	2.12	3.2+	24	$\text{Si}_3\text{N}_4$	62.5	
16-73	2.1	-	24	$\text{Si}_3\text{N}_4$	62.5	

All batches were dry ball milled and except as noted contained 88 wt/%  $\text{Si}_3\text{N}_4$ , 8 wt/%  $\text{Y}_2\text{O}_3$ , 4 wt/%  $\text{Al}_2\text{O}_3$  with 2 wt/% stearic acid added.

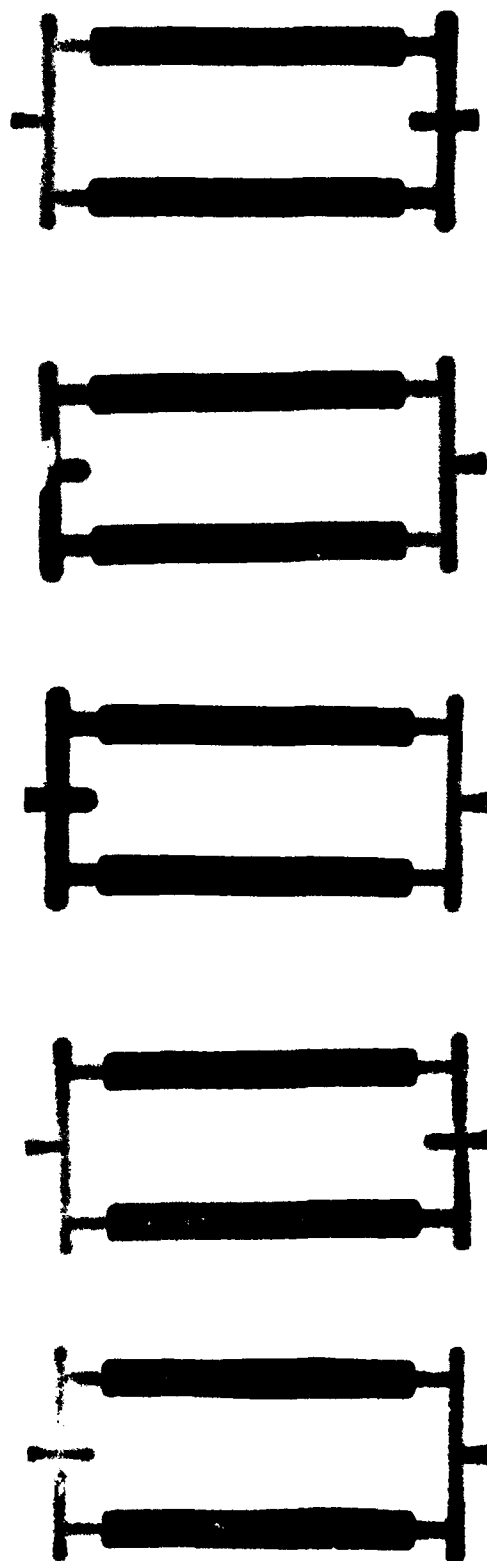


figure 12. X-Ray Radiograph Demonstrating Flaws in  
Injection Run No. 12127xx

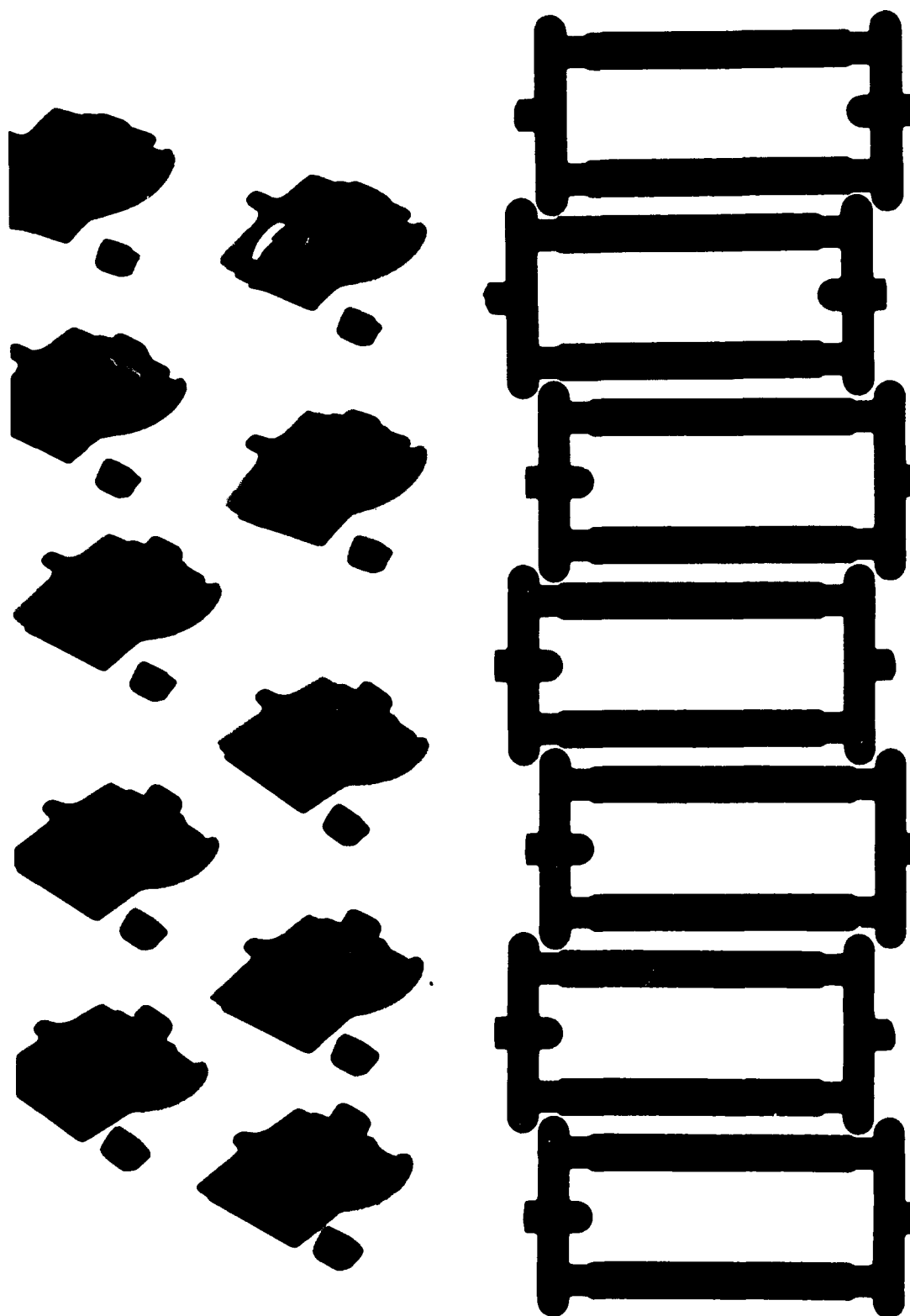


Figure 13. X-Ray Radiograph Showing Injection-Molded Stator Vanes and Test Bar Sets Using Batch 116-25

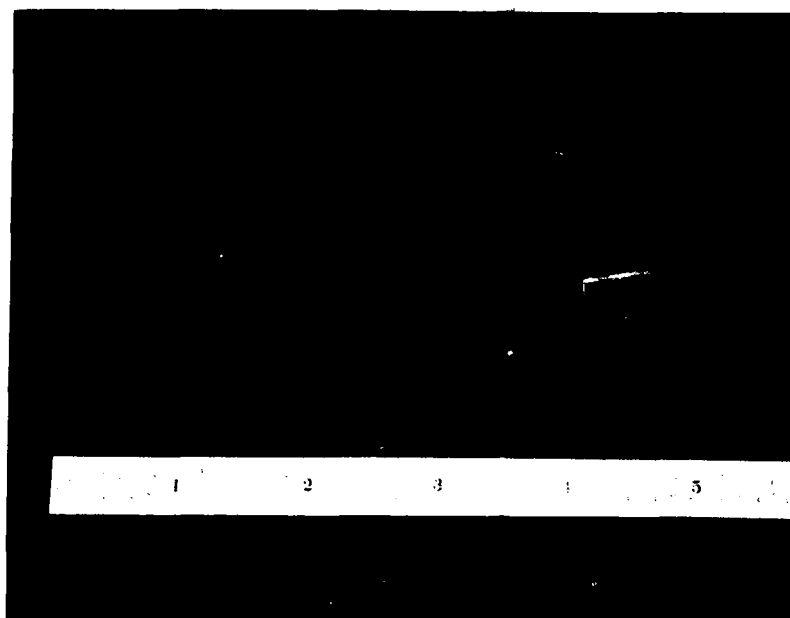


Figure 14. As-Injected Stator Vane and Test Bars

Excellent quality injection-molded vanes and test bars were made with both the steel and  $\text{Si}_3\text{N}_4$  media-milled powders. Injection details that appeared near optimum for all of the batches are shown in Table 7.

TABLE 7  
INJECTION DETAILS FOR VANES AND TEST BARS

Injection Machine: Arburg 221E-150			
Part Injected: TPE331-C turbine second stage stator vane and two associated MOR test bars			
Machine Settings:			
Feed zone	344°K	Injection pressure	100 MPa
Plastic zone	350°K	Mold clamp	15 to 36 sec
Nozzle zone	350°K	Shot length	5 cm
Injection speed	Max.	Mold temp	301°K
Injection time	5 sec		

A difficulty that had not been experienced with previous batches occurred with both steel and  $\text{Si}_3\text{N}_4$  media-milled material. It was extremely difficult to remove the vanes from the tooling. During the early injection runs, approximately half of the parts were destroyed during removal since the powders produce a very rigid compact. The injection parameters were varied in an attempt to enhance part release. The only change that was effective was to reduce the mold clamp time from 36 sec to less than 18 sec. This apparently prevents complete chilling and rigidization of the part, therefore allowing it to yield slightly during withdrawal.

Vaness and test bars resulting from this effort were subjected to further processing. (Refer to Para 3.5.)

#### 3.3.2.1 Injection Molding, 16-60 SN3512 Based Mix

An injection blend was prepared by hot mixing as-received 3512 with LN-27-266-2 organic binder. This blend (16-60) contained 14 weight/percent organic with a resulting 63.7 volume/percent inorganics.

The injection molding trials were made by using a multiple test bar tool that produces four 6.35 by 3.175 by 76.2 mm modules of rupture specimens per injection. The optimum machine settings for the test bar tool on the Arburg 221E-150 are shown in Table 8.

TABLE 8

OPTIMUM MACHINE SETTINGS FOR TEST BAR INJECTION

Feed zone	339°K	Injection speed	5 (max.)
Plastic zone	344°K	Injection time	5 sec
Nozzle zone	344°K	Clamp time	36 sec
Mold	301°K	Injection pressure	95.6 MPa

A total of 104 specimens were made under these conditions. The parts were very sound without internal or external molding flaws that could be detected by visual examination or conventional radiography. The bars also had excellent green strength, were easy to remove from the molding tool, and had smooth, shiny surfaces. They were subjected to binder extraction and used for the evaluation of the 3512 material sinterability.

#### 3.3.2.2 Injection Molding, 16-43 SN502 Baseline Mix

In this series, the injection conditions were the same as described in para. 3.3.2.1. The same tool was also used to inject modulus of rupture test specimens. Figure 15 shows the tool in place in the Arburg.

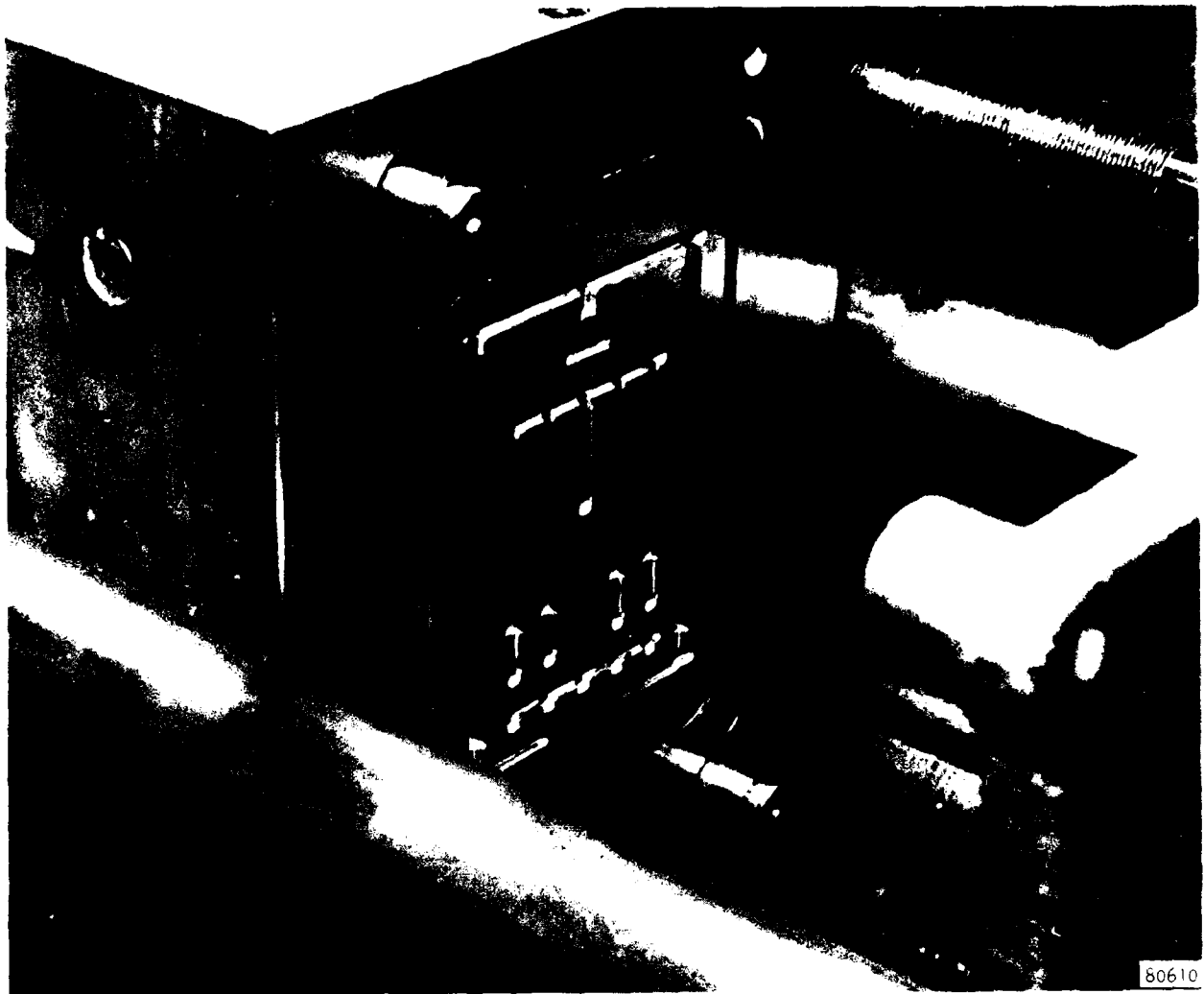


Figure 15. Test Bar Tool in Position in Arburg Injection Machine

Excellent quality parts were produced with both the 16-43 and 16-60 (see Table 6) compositions. This series of experiments revealed that a high wear rate occurred on the screw tip and valve assembly during the screw rotation (plasticizing cycle) and carriage withdrawal. This rapid wear rate occurred during the injection of both materials. It was the only wear problem found, and the cause was not determined.

### 3.3.3 Composition 16-60 Processing--Powder Preparation

This material, GTE 3512, was reportedly in a ready-to-form condition as received. Early measurements of uniaxially cold-pressed packing density and sintering results, however, indicated additional treatment (milling) might be beneficial. In particular, the existence of a threshold green density greater than that being realized was believed to be required for sintering to occur. This was verified by communication with GTE, who suggested that the minimum green density had to be greater than 2.0 gm/cc. Consequently, dry-ball milling was used to improve the compactability of the powder. The powder was milled in a rubber-lined jar mill for 22 hr. A powder charge of 200 gm was used with 2.2 kg of high density (3.19 gm/cc) silicon nitride grinding media.

The effect of ball-milling on the green density of cold-pressed discs is given in Table 9. It was also noted during this study that the green density of discs made with milled 3512 appeared to be independent of the forming pressure. Unlike most common ceramic powders that exhibit an increase in density with increasing pressure, this powder produced almost the same green density at various pressures in the 24 to 103 MPa range. (See Table 10.)

TABLE 9

BALL-MILLING EFFECT ON GREEN DENSITY OF COLD-PRESSED DISCS

Forming Pressure		Green Density, gm/cc	
MPa	ksi	As received	Milled 22 hr
103	15	1.77	2.21
138	20	1.85	--

TABLE 10

PRESSING PRESSURE VS DENSITY FOR BALL MILLED AND  
COLD PRESSED 3512  $\text{Si}_3\text{N}_4$

Pressure		Density, gm/cc
MPa	ksi	
24	3.5	2.18
34.5	5	2.21
69	10	2.19
103	15	2.20

### 3.3.4 Composition 16-43 Processing

#### 3.3.4.1 Powder Preparation

The 700-gm ball mill batches were prepared by combining the various materials as listed in Table 11.

Each batch was milled 24 hr in a 20-cm ID rubber-lined mill with 2.2 kg of  $\text{Si}_3\text{N}_4$  cylindrical grinding media. Mills were discharged over a coarse screen to separate media and powder.

TABLE 11  
COMPONENTS FOR 700-gm BATCH OF COMPOSITION 16-43

Material	Description	Weight, percent	Weight, gm
$\text{Si}_3\text{N}_4$	GTE Sylvania type 502	88	616
$\text{Y}_2\text{O}_3$	Molycorp 5600	8	56
$\text{Al}_2\text{O}_3$	Union Carbide Linde-A	<u>4</u>	<u>28</u>
	Total inorganic	100	700
Stearic acid	MCB practical grade	2	14

The effect of milling time and the use of stearic acid on particle packing was determined. Figure 16 shows a gradual increase in green compact density with time; also, there is a significant increase in green density as a result of the addition of stearic acid.

Two mill batches were dry-blended together to form an injection mix. Blending of the organic binder and powder was accomplished by preheating the sigma bladed mixer to 394°K, melting the desired amount of binder in the mixer, and then slowly adding the inorganic powder. The powder also had been preheated to 394°K. After one-half hour of mixing, the heater was shut off and the batch was allowed to cool with the mixer running. The batch was removed when it had thickened to the point where it could be removed readily from the mixer chamber. After final cooling to room temperature, the blend was pelletized.

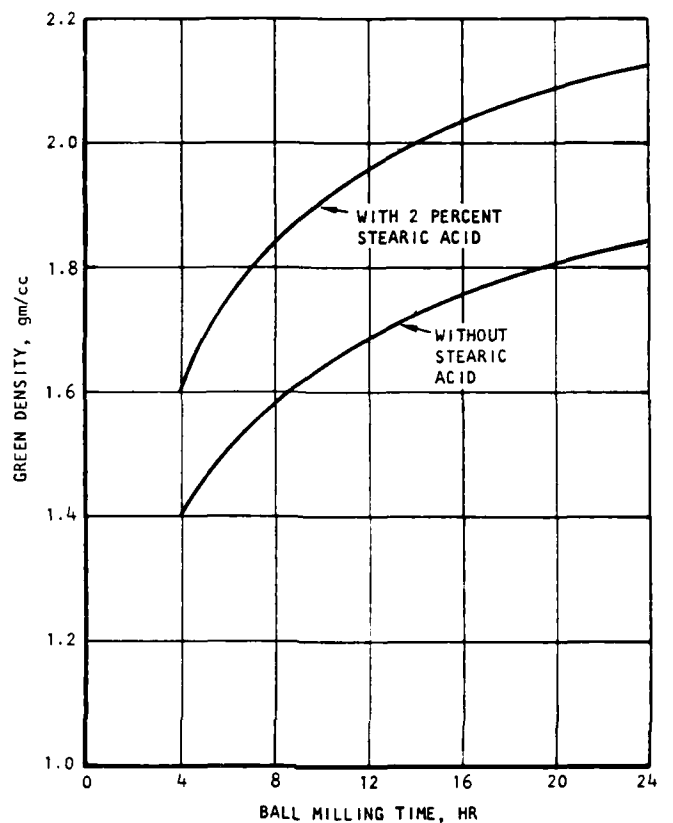


Figure 16. Cold Pressed Green Density vs Milling Time

### 3.4 INJECTION MOLDING

#### 3.4.1 Die Selection

Three injection molding dies were selected from those available for use on this program. Initially an AiResearch tool (a spiral mold die, per ASTM test method D-3123-72) was used to optimize solids/binder ratios, mixing conditions, injection parameters, etc., for the initial compositions. A photograph of this high pressure die in the Arburg Model 221E-150 injection molding machine is shown in Figure 17.

The second injection molding die, which had been built under DARPA/NAVSEA Contract N00024-76-C-5352, was used on this program with the consent of DARPA. This tool, shown in Figure 18, produces two test bars and one second-stage stator vane for the AiResearch TSE 331C-1 1040 hp ceramic turbine engine. The product of a typical "shot" is shown in Figure 19. The third tool, producing four MOR test bars per injection, is shown in Figure 15.

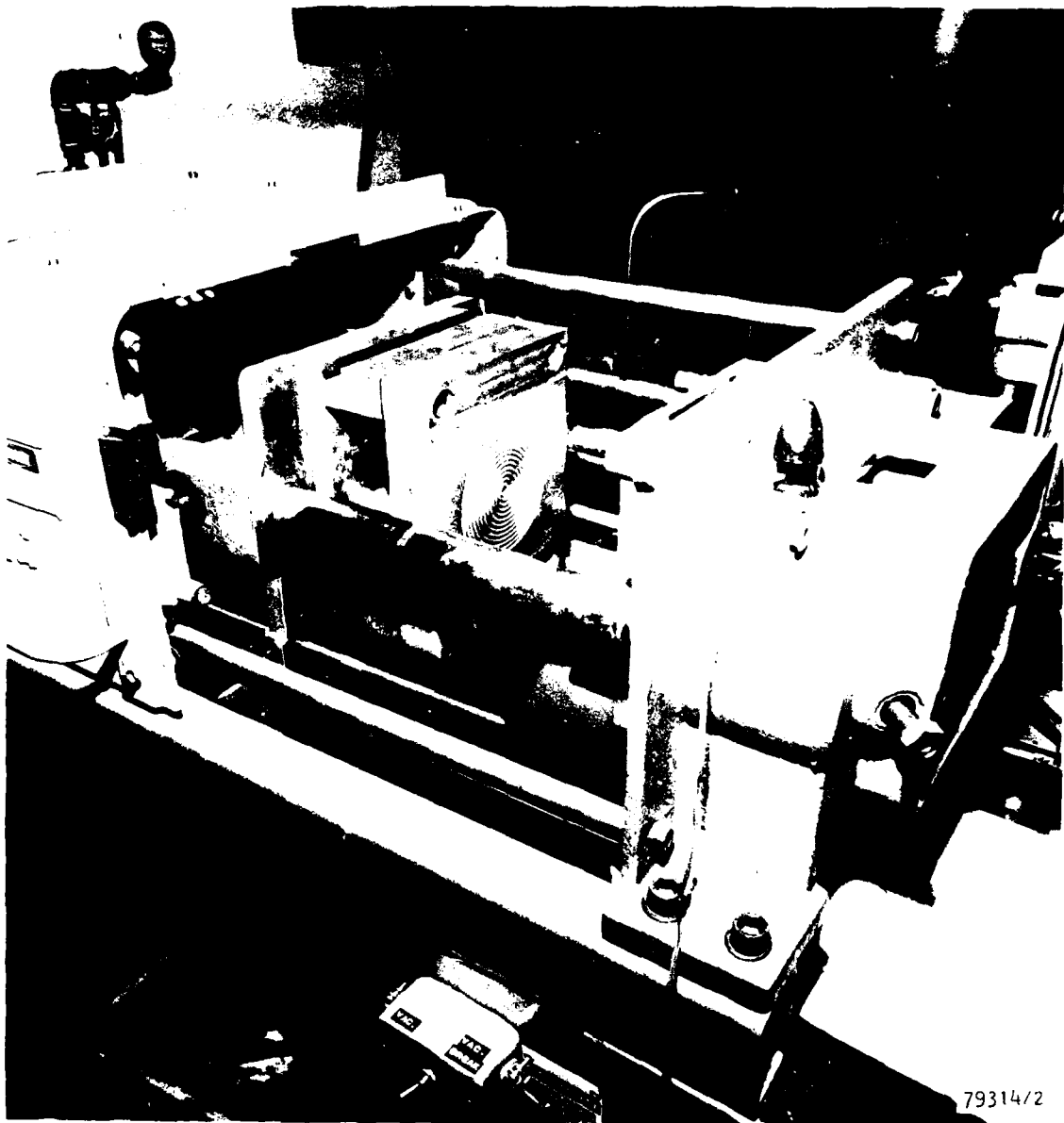
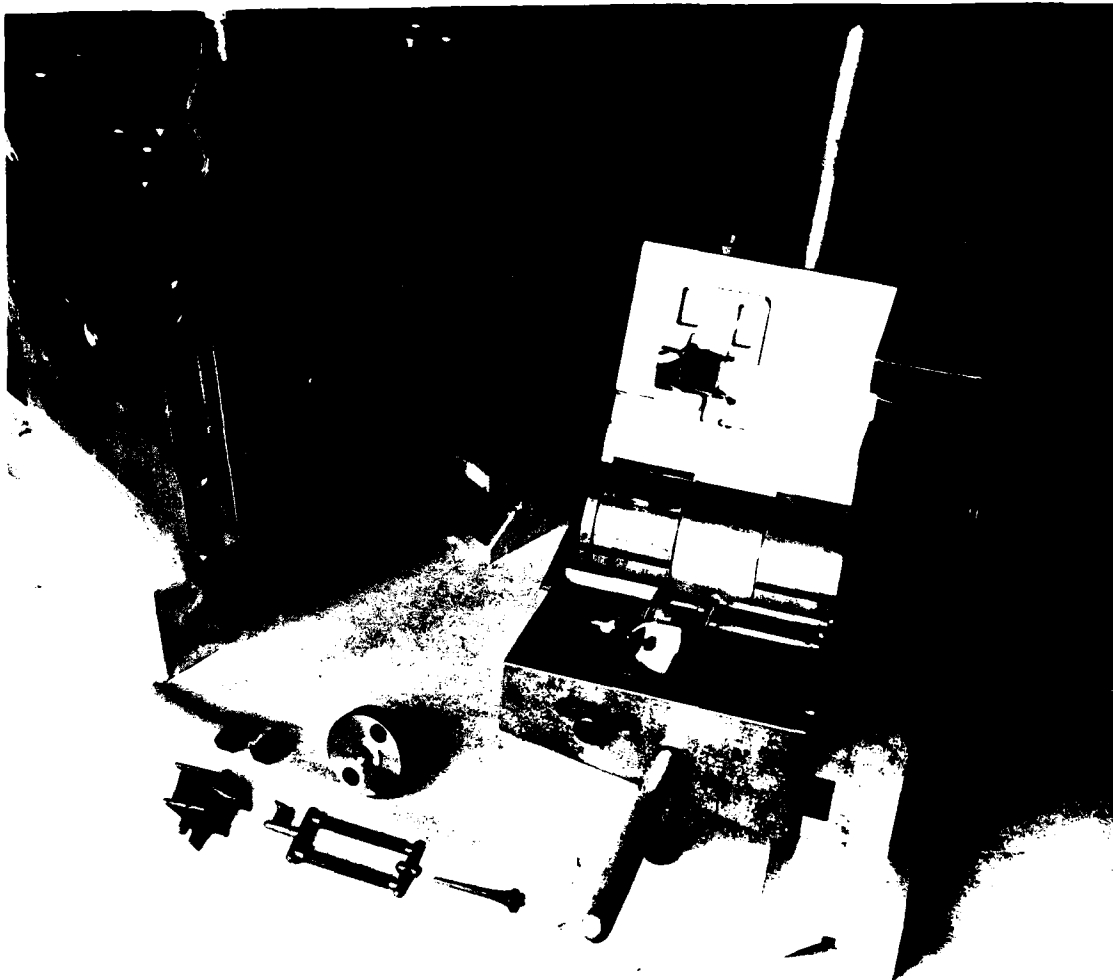
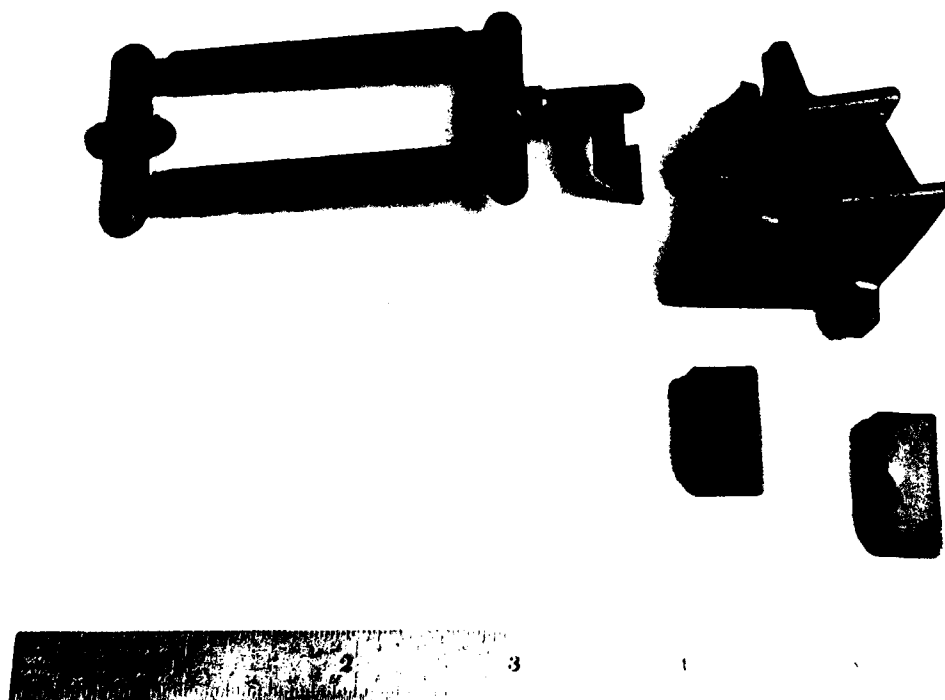


Figure 17. Injection Molding Die T-62042-1 Installed in Injection Molding Machine



78699-1

Figure 18. Injection Molding Die T-62044



78655-9

Figure 19. Parts Produced with Die T-62044 in Typical Molding Operation

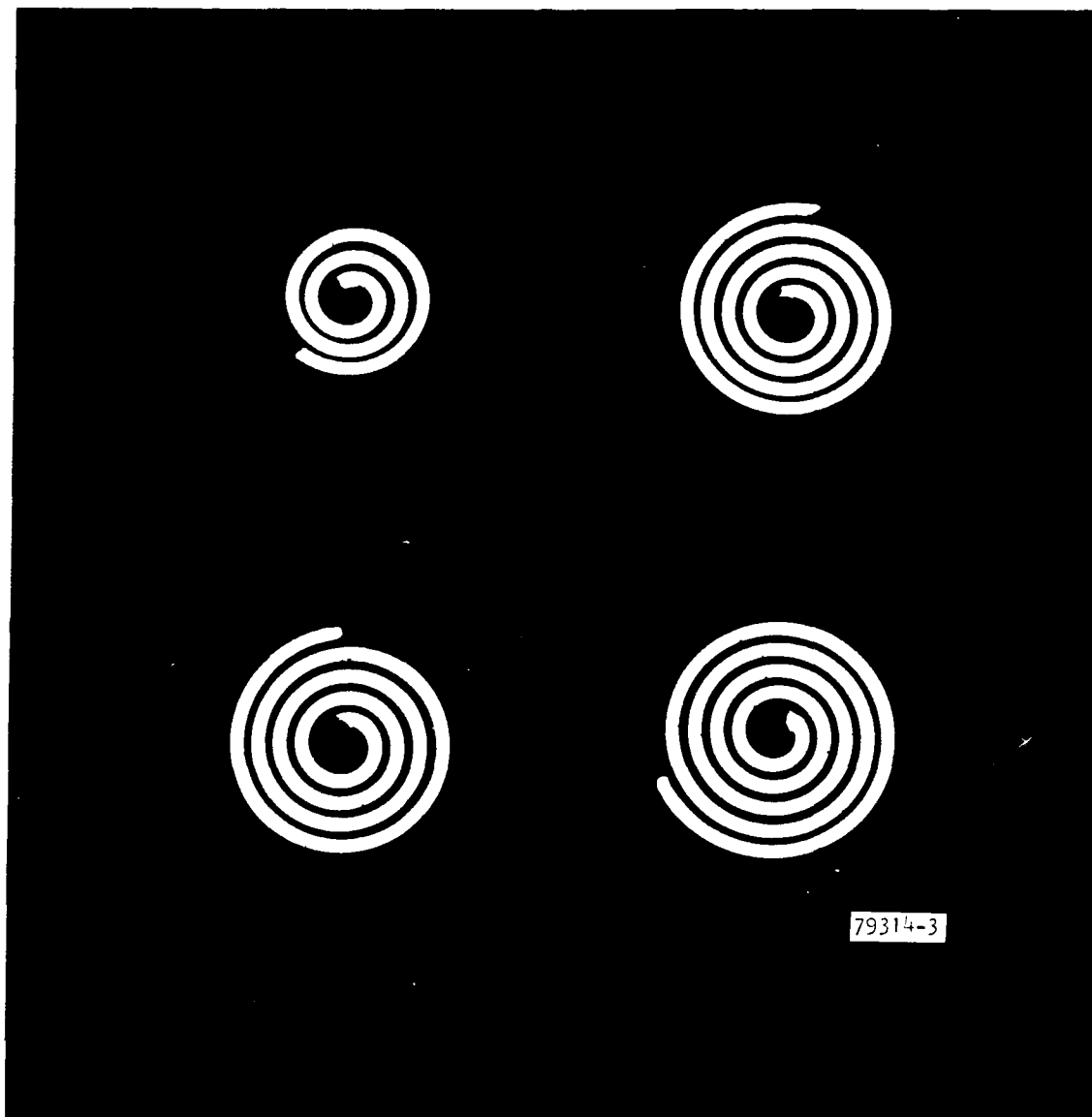
### 3.4.2 Injection Molding

The first two injection molding experiments were conducted using the ASTM spiral flow mold tooling. Experiment No. 1 was performed using batch 116-1. Experiment No. 2 was performed using batch 116-2 (see Table 4). Table 12 describes the injection molder parameter setup for each experiment. The results of the series of injection experiments are shown in Figure 20. While flow of this magnitude is less than desirable, it was determined that this batch could be used for subsequent testing of the test bar/vane tool set.

Experiment No. 2 (batch 116-2) produced the longest spiral, approximately 58 cm (23 in.) long. The longest spiral obtained for experiment No. 1 was 45 cm (17-1/2 in.). Past experience has indicated that flow of this magnitude is sufficient to successfully fill the test bar/stator vane ARPA tool.

TABLE 12  
INJECTION MOLDING PARAMETERS

Injection Molding Control Setting	Experiment No. 1	Experiment No. 2
Feed zone temperature	350°K (170°F)	359°K (170°F)
Plasticizing zone temperature	355°K (180°F)	355°K (180°F)
Nozzle temperature	364°K (195°F)	364°K (195°F)
Injection speed	No. 5	No. 5
Injection time, sec	5	2.5
Injection pressure	124 MPa (1800 psi)	124 MPa (1800 psi)
Clamp time, sec	36	36
Mold temperature	295°K (72°F)	295°K (72°F)
Holding pressure	12.4 MPa (1800 psi)	12.4 MPa (1800 psi)
Shot size, cm	2.5 to 5.5	2.5 to 5.5



1 cm

Figure 20. Results of Injection Molding Experiment using Spiral Flow Mold Tooling; Batch 116-1 on Left and 116-2 on Right

### 3.5 BINDER EXTRACTION

Binder extraction is a critical step in the process, as shown in Figure 21. The vane on the left, which is badly blistered, is the result of a temperature controller malfunction that caused an overtemperature excursion from the program. The normal furnace cycle used is a linear 24-hr ramp to 522°K (249°C) in vacuum with the parts imbedded in activated charcoal. The stator vane shown on the right in Figure 21 is the product of this cycle.

Binder extraction parameters (rate of temperature rise and cooldown) for the organic system used had been established prior to the onset of this program. Therefore, no additional work was done. Figure 22 is a photograph of several ready-to-sinter stator vanes with their associated test bars from batch 116-25.

The binder extraction furnace is a vacuum/pressure vessel, 1.22 m (4 ft) in diameter by 1.83 m (6 ft) long, suitable for backfilling with nitrogen after extraction of the binder system (which is normally conducted under vacuum). During extraction, specimens are buried in trays of activated charcoal. The trays are transferred into a nearby glove box where the parts are removed from the charcoal and placed on reaction-bonded silicon nitride plates for the sintering operation. While recycling of the charcoal might be possible, fresh material was used for each run to prevent contamination.

A change was made in this process step during the third quarter of the program as a result of the findings on a related program. It was determined that the maximum temperature obtained during the extraction cycle was marginal and that in some cases incomplete binder removal occurred. Consequently, the peak temperature was raised from 522°K (249°C) to 578°K (305°C). No evidence of residual carbon has been noticed since then.

### 3.6 SINTERING

Previous experience with the Sylvania powders had shown that sintering must be done under a positive nitrogen atmosphere because of significant vapor pressure in the temperature range required for sintering. Therefore, the vacuum/pressure furnace shown in Figure 23 was modified for use on this program. It is induction heated by the 100 kw, 3000 Hz motor generator set visible in the left background of Figure 23. The furnace chamber is a graphite susceptor 14 cm (5-1/2 in.) ID by 30.5 cm (12 in.) high. All sinterings were at 2 atmospheres nitrogen pressure, which appeared to be sufficient for this program. An important provision is a vacuum outgassing step, reported by GE researchers as necessary to remove residual chlorides contained in some  $\text{Si}_3\text{N}_4$  powders.

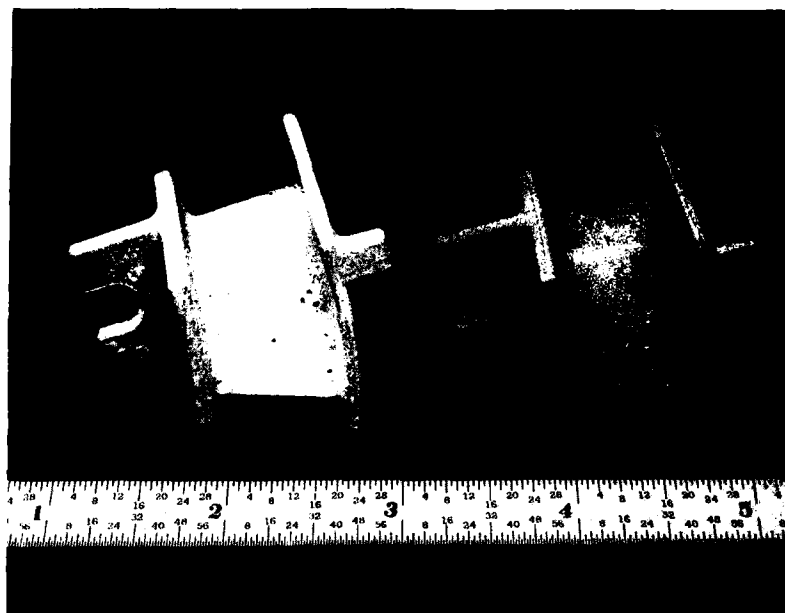


Figure 21. Results of Improper (Left-hand Vane) and Proper (Right-hand Vane) Binder Extraction

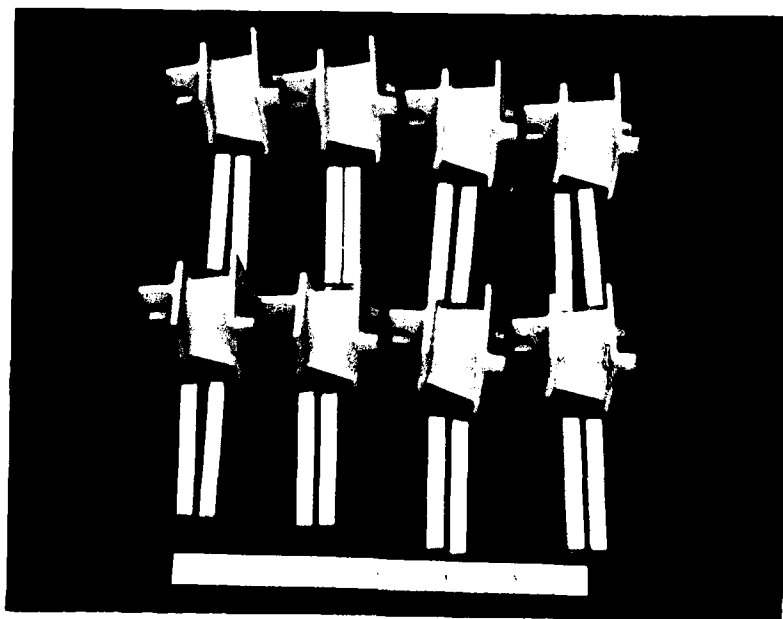


Figure 22. Dewaxed Vanes from Batch 116-25 (70 percent solids) Ready to Sinter

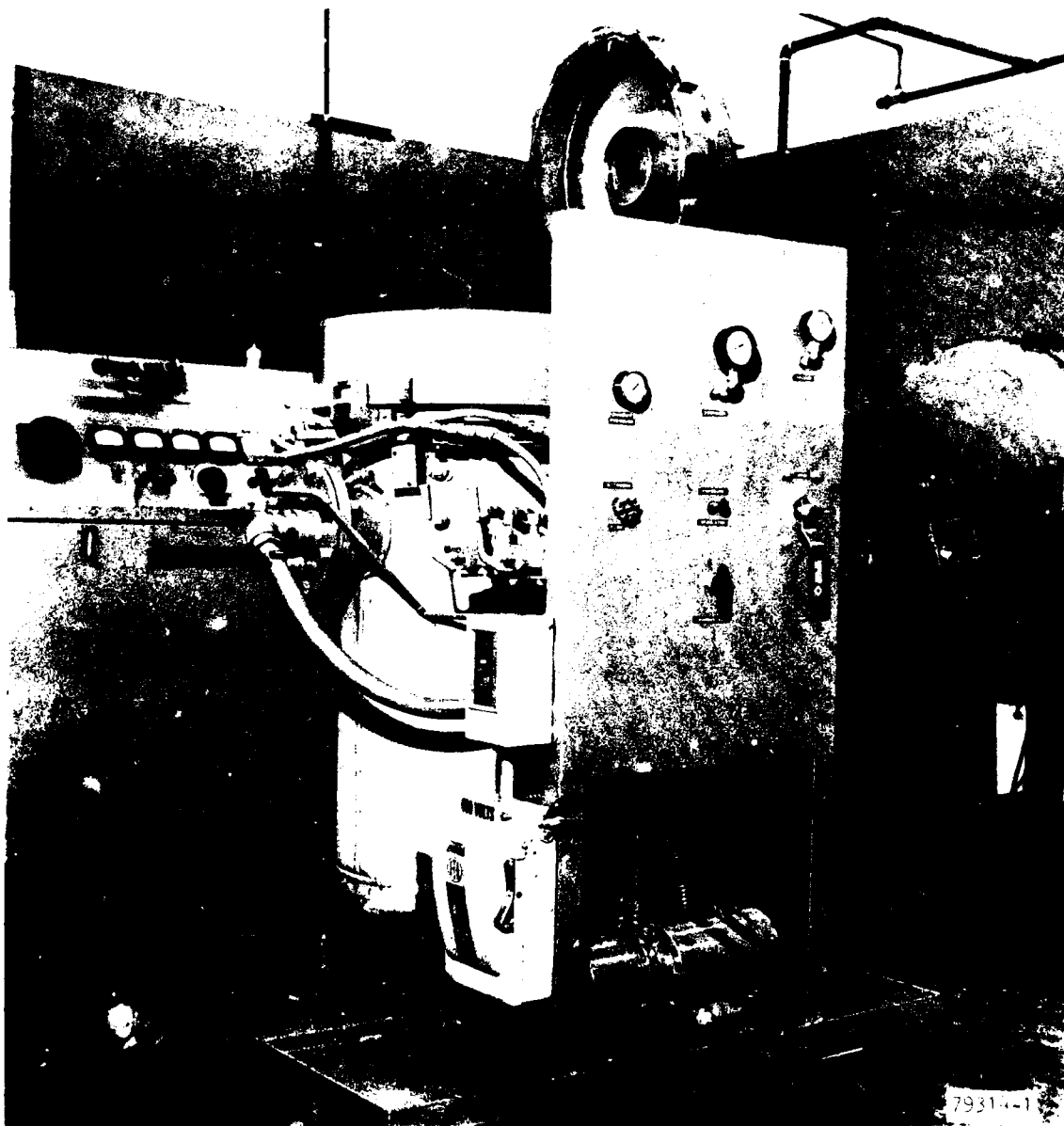


Figure 23. Vacuum/Pressure Furnace (Right) and Motor Generator Set (Left)

### 3.6.1 High-Temperature Sintering Runs

The first series of high-temperature sintering runs performed are listed in Table 13.

The highest sintered densities (3.06 gm/cc) achieved in this series were with sample materials that had been milled in the alumina mills with alumina grinding media, despite the fact that the green densities ( $\rho_g$ ) were lower than those achieved with steel milled material. Scanning electron micrographs (SEM) of polished surfaces of the alumina milled material (run No. 2) are shown in Figure 24. The pore size is very small compared with the results shown by other workers (Ref. 2).

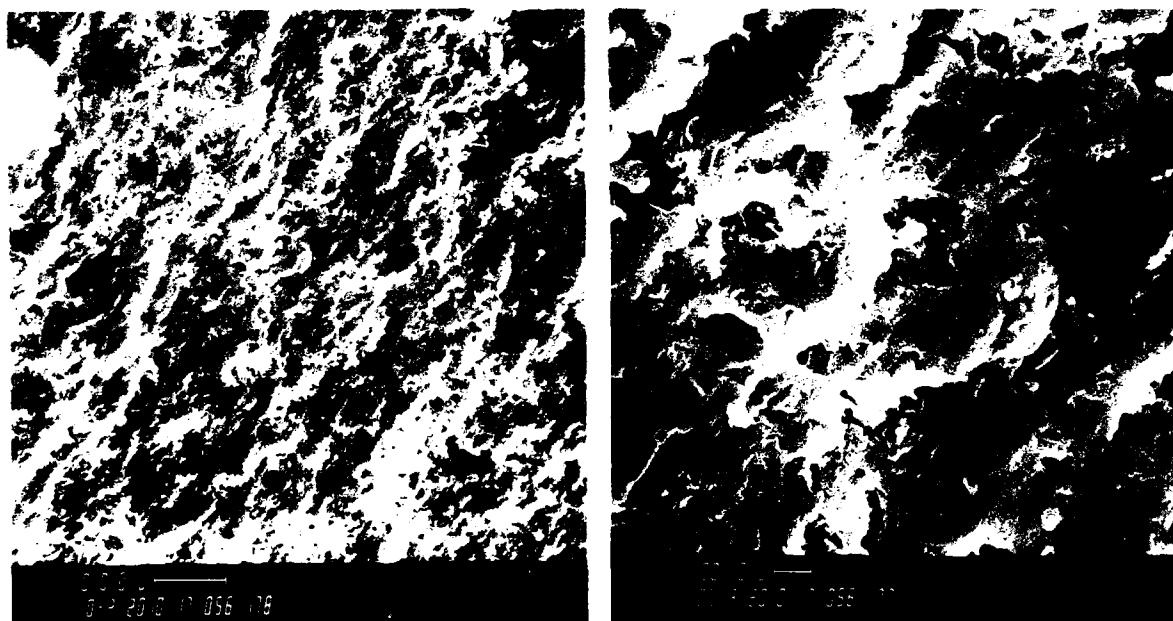


Figure 24. Sintered  $\text{Si}_3\text{N}_4 + 4$  Weight/Percent  $\text{Y}_2\text{O}_3$ , 1923°K, 1 hr

Figure 25 shows the difference in shrinkage of sintered stator vanes made with  $\text{Al}_2\text{O}_3$  vs steel milled powders. The vane on the left was made with batch 116-2 ( $\text{Al}_2\text{O}_3$  media) and sintered to 3.03 gm/cc. The vane on the right was from batch 116-25 (steel media) and sintered to 2.2 gm/cc.

TABLE 13  
SINTERING RUN PARAMETERS

Run No.	Purpose	Configuration	Cycle(1)
1	Furnace checkout	None	Ambient to 1753°K, 2-1/2 hr, 0.2 MPa
2	Furnace checkout Simulate sintering run	Injection sprue	1923°K, 1 hr
3	Test sintering	Vanes and test bars	1973°K, 1 hr
4	Injected part sintered	Vanes and test bars	1923°K, 1 hr
5	Injected part sintered	Vanes and test bars	1923°K, 1 hr
6	Injected part sintered	Vanes and test bars	1923°K, 1 hr
7	Three batch comparison, effect of closed sagger	Discs(2)	1873°K, 1 hr
8	70 v/o solids injection evaluation	Vanes and test bars	1873°K, 3 hr

(1) All firings ambient to 1373°K in vacuum, then pressurized to 0.21 MPa nitrogen.

(2) Dry-pressed discs without binder.

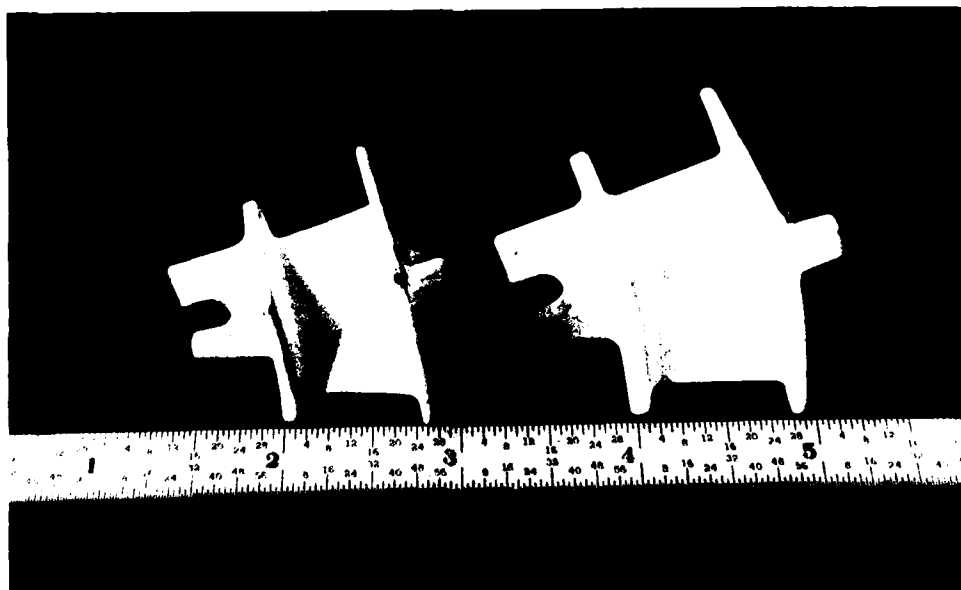


Figure 25. Sintered Stator Vanes

During the first few runs, a problem was experienced with the optical temperature measurements. A fibrous deposit accumulated in the susceptor cover pyrometer sight hole, which caused a lower-than-actual temperature readout and caused the abortion of those particular tests. The problem was resolved by enlarging the sight hole.

Another problem that emerged was vapor emission "smoke" during the heat up portion of the cycle, which made the accuracy of optical temperature measurements suspect. However, the vapor eventually disappeared, and the accuracy of the temperature measurements could be verified.

To ensure greater accuracy of temperature readout and to verify the optical measurements, a molybdenum-clad, BeO-insulated, tungsten-rhenium thermocouple was installed in the sintering furnace. Very close (5°K) agreement was found between the two.

It was expected that firing parts in a closed silicon nitride sagger would inhibit the fibrous growth covering the optical sight hole. A reaction bonded silicon nitride sagger and cover were made, but later found to be unnecessary for the intended purpose as the enlarged hole in the susceptor had effectively reduced the problem of obstruction. However, their use does provide a real benefit. Dry-pressed discs fabricated from batch 116-2 were sintered, some inside and some outside of the sagger. The weight loss of parts inside the sagger was typically on the order of 1.3 percent, whereas parts fired outside the sagger exhibited weight losses on the order of 4 percent. Figure 26 shows the discs after sintering. Parts inside the sagger exhibited no whisker growth, whereas parts outside exhibited considerable whisker growth due to volatilization. Work reported by other investigators (Ref. 2) revealed similarly high weight losses under similar time/temperature conditions as occurred outside the sagger.



Figure 26. Dry-Pressed Discs Sintered Inside and Outside of  $\text{Si}_3\text{N}_4$  Sagger

### 3.6.2 Results of XRD Analyses

To determine the phase distributions in the starting powders, quantitative X-ray diffraction (XRD) analysis techniques were used on a mixture of alpha-Si<sub>3</sub>N<sub>4</sub>, beta-Si<sub>3</sub>N<sub>4</sub>, Si<sub>2</sub>ON<sub>2</sub>, Si, SiO<sub>2</sub> (alpha-cristobalite), and SiC. After investigation of the calculation techniques of Mencik and Short at Ford Motor Co. (Ref. 7) and of Gazzara and Messier of AMMRC (Ref. 8), the Ford technique was adopted because of its relative simplicity. Neither of the techniques treats mixtures containing Al<sub>2</sub>O<sub>3</sub> or Y<sub>2</sub>O<sub>3</sub>, and neither considers the amorphous content.

Calculation of the phase concentration from the peak heights on the X-ray patterns for the as-received GTE 502 Si<sub>3</sub>N<sub>4</sub> powder gave 97.1 percent alpha-Si<sub>3</sub>N<sub>4</sub>, 2.6 percent beta-Si<sub>3</sub>N<sub>4</sub>, and 0.2 percent Si. The diffractometer scan is shown in Figure 27. A Norelco diffractometer was used, with CuK $\alpha$  radiation and a graphite crystal monochromator.

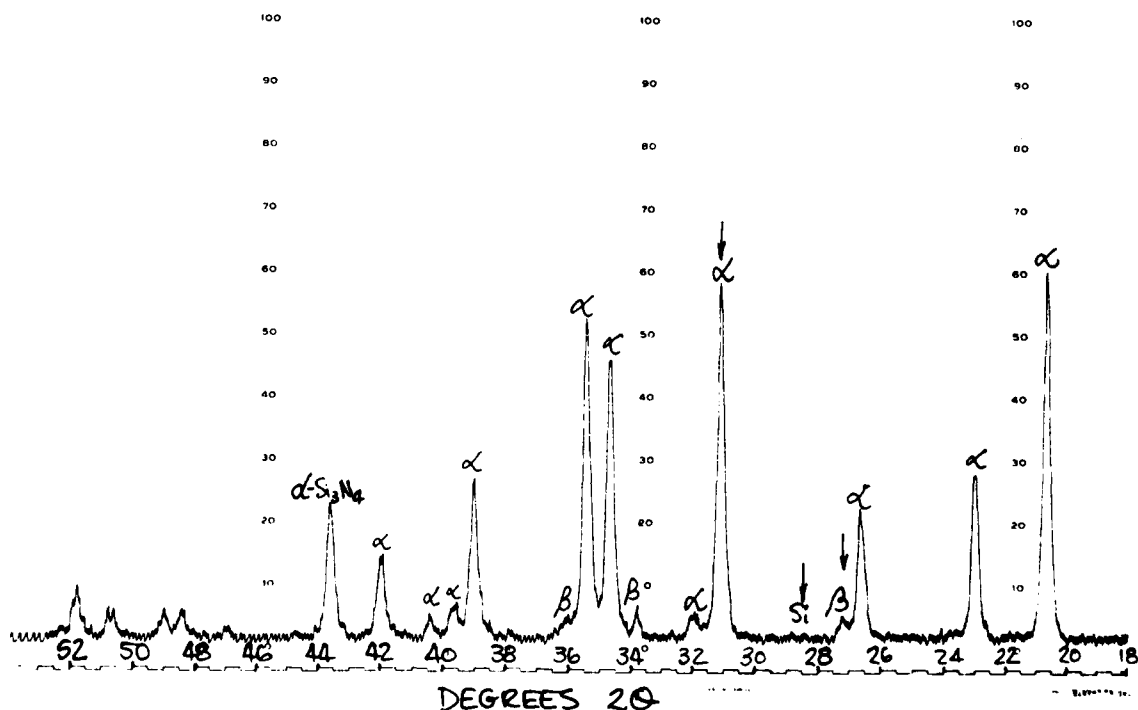


Figure 27. X-Ray Diffraction Pattern of As-Received GTE 502 Si<sub>3</sub>N<sub>4</sub> Powder

Qualitative XRD analysis of GTE 502 powder with 4 weight/percent  $Y_2O_3$  added, milled in an  $Al_2O_3$  mill with  $Al_2O_3$  media, injection molded, and dewaxed at  $522^\circ K$  is shown in Figure 28. Peaks of alpha  $Si_3N_4$ , beta  $Si_3N_4$ ,  $Y_2O_3$ , and  $Al_2O_3$  are all present. The XRD pattern of the same material after sintering for 1 hr at  $1923^\circ K$  is shown in Figure 29. It is apparent that the  $Al_2O_3$ ,  $Y_2O_3$ , and alpha  $Si_3N_4$  patterns have all disappeared. The only crystalline phase present in significant quantities is a hexagonal phase with d-spacings similar to those of beta- $Si_3N_4$ . Therefore, it is identified as the beta solid solution. Approximate lattice parameters calculated from Figure 29 are  $a_0 = 7.65\text{\AA}$  and  $c_0 = 2.95\text{\AA}$ . According to data presented by Jack (Ref. 3), and assuming the  $Y_2O_3$  does not dissolve in the beta, these lattice parameters would correspond to the stoichiometry  $Si_4Al_2O_2N_6$ , or about 19 weight/percent Al. These data indicate that the final product is not  $\beta$ - $Si_3N_4$ , but rather is Sialon (Ref. 3).

### 3.6.3 Additional Sintering Studies

Sintering studies during the next period involved 18 compositional or pre-conditioning variations, and 21 sintering runs. Most of the compositions studied were in the Y-Si-Al-O-N system. Four other tests with 6, 8, 10, and 12 weight/percent  $Y_2O_3$  added, but with no  $Al_2O_3$  resulted in inadequate sintering even at  $2023^\circ K$  for 4 hr. A summary of the compositions studied, milling, average green and fired densities, and sintering cycles is presented in Table 14.

The composition of the first nonalumina-milled batch to achieve a sintered density greater than 3.0 gm/cc consisted of GTE 502  $Si_3N_4$  plus the addition of 8 and 4 weight/percent  $Y_2O_3$  and  $Al_2O_3$ , respectively. Dry-pressed discs of this material had the following sintering behavior:

Temp, $^\circ K$	Time, hr	Density gm/cc	Theoretical Density, percent
1923	2	2.87	87
1998	2	3.11	94
1998	4	3.16	95
2023	3	3.24	98

The importance of  $Al_2O_3$  on sinterability is demonstrated in the test series containing 8 weight/percent  $Y_2O_3$  and various levels of  $Al_2O_3$ . The sintering results are illustrated in Figure 30 and show sintered density increasing from 2.0 gm/cc without  $Al_2O_3$  to 3.1 gm/cc with 4 percent  $Al_2O_3$ . All samples were cold pressed and sintered at  $1998^\circ K$  for 2 hr.

The sintering behavior of the 16-43 composition is plotted in Figure 31 as a function of sintered density vs time at  $2023^\circ K$ . The theoretical density calculated for the mixture of inorganic components is 3.35 gm/cc.

Modulus of rupture (MOR) measurements by four point bending test were made on two injection molded sets of sintered specimens, both of the composition 88 wt/%  $Si_3N_4$ -4 wt/%  $Al_2O_3$ -8 wt/%  $Y_2O_3$ . One was sintered at  $2023^\circ K$  for 1.5 hr

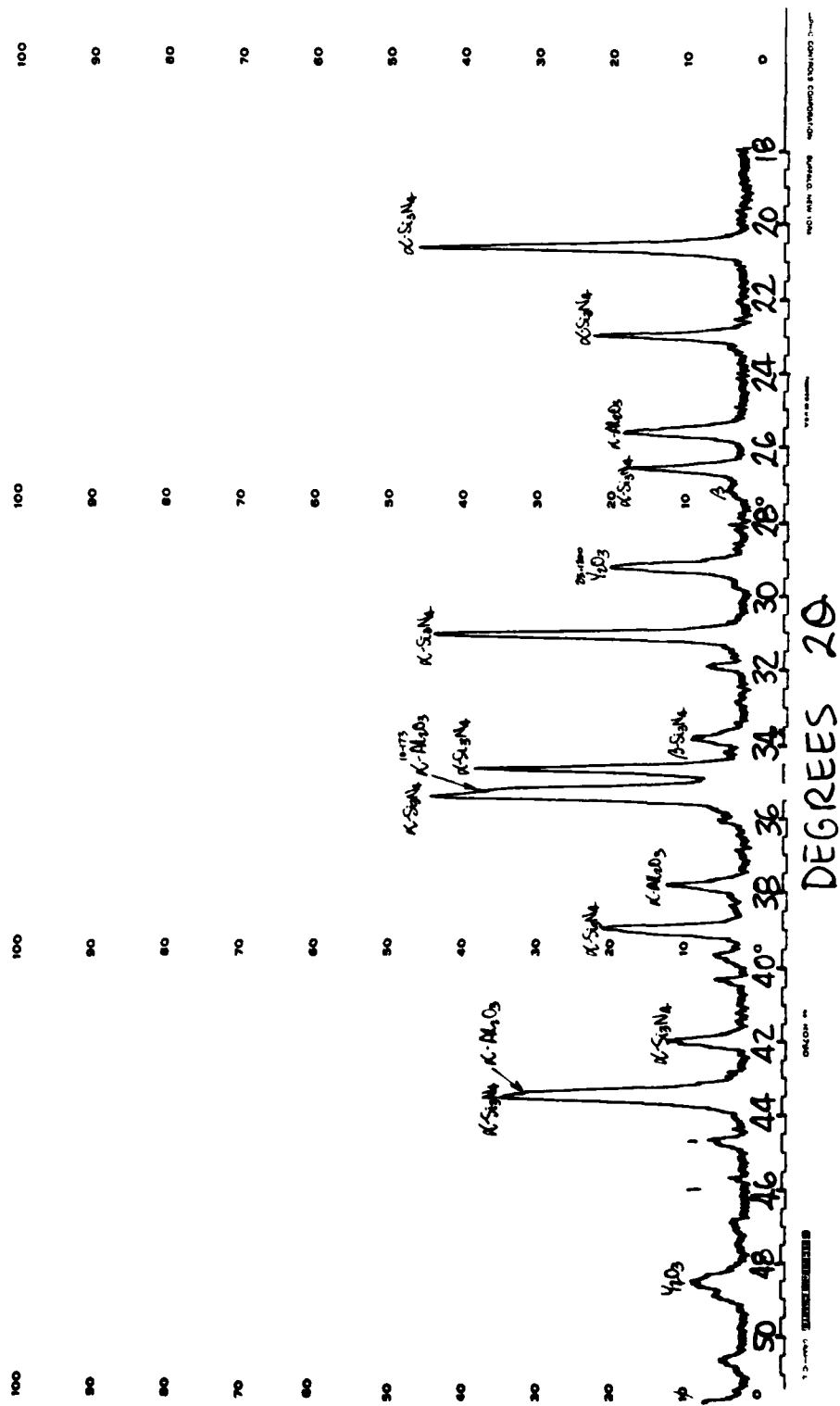


Figure 28. X-Ray Diffraction Pattern of GTE 502  $\text{Si}_3\text{N}_4$  Powder with 4 Weight%  $\text{Y}_2\text{O}_3$  Added (Milled with  $\text{Al}_2\text{O}_3$  media, injection molded, dewaxed.  $\text{CuK}\alpha$  radiation monochromator.)

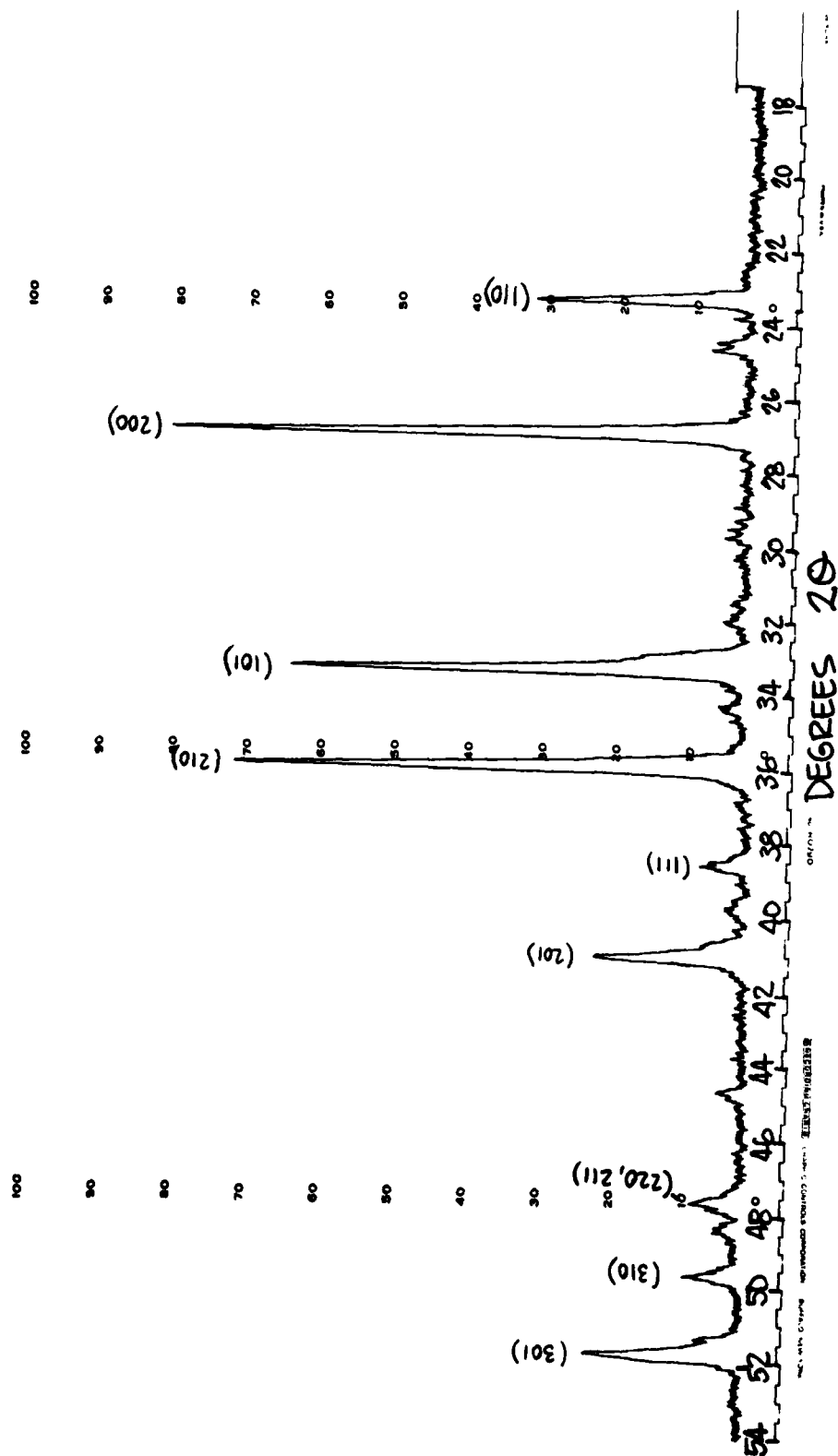


Figure 29. X-Ray Diffraction Pattern of Material from Figure 27 after Sintering (CuK $\alpha$  radiation, monochromator. Miller indices are shown, based on a hexagonal lattice.)

TABLE 14  
SINTERING STUDY SUMMARY

Batch	Composition, Percent	Milling Media	Milling Time, hr	Green Density, gm/cc	Fired Density, gm/cc	Sintering Temperature, K°	Sintering Time, hr
16-29	4Y 2A 2St*	Steel	16	2.07	2.30	1873	2
16-33	4Y 1A 2St	Si <sub>3</sub> N <sub>4</sub>	24	1.96	2.18	1873-1923	2
16-34	4Y 2A 2St	Si <sub>3</sub> N <sub>4</sub>	24	1.48			
16-37	4Y 2A 2St	Si <sub>3</sub> N <sub>4</sub>	24	1.95	2.23	1973	2
16-38	4Y 4A 2St	Si <sub>3</sub> N <sub>4</sub>	24	1.97	2.54	1923	2
16-33A	6Y 4A 2St	Si <sub>3</sub> N <sub>4</sub>	25	1.99	2.70 3.00	1923 2023	2 2
16-33B	8Y 4A 2St	Si <sub>3</sub> N <sub>4</sub>	26	1.98 2.02 2.00	2.87 3.11 3.16	1923 1998 1998	2 2 4
16-41	SN512 + 6Y + 2 St	Si <sub>3</sub> N <sub>4</sub>	1	2.07	1.92	1923	2
16-40A	8Y	Si <sub>3</sub> N <sub>4</sub>	24	1.80	2.01	1998	2
16-40B	8Y 0.25A	Si <sub>3</sub> N <sub>4</sub>	25	1.82	2.06	1998	2
16-40C	8Y 1A	Si <sub>3</sub> N <sub>4</sub>	26	1.77	2.19	1998	2
16-40D	8Y 2A	Si <sub>3</sub> N <sub>4</sub>	27	1.77	2.46 2.78	1998 1998	2 5
16-43	8Y 4A 2St	Si <sub>3</sub> N <sub>4</sub>	24	1.94	3.07 3.24**	1998 2023	2 3**
16-44	8Y 4A 2St	Steel	16	2.07	3.13 3.20**	1998 2023	5 4**
16-50A	10Y 0A 2St	Si <sub>3</sub> N <sub>4</sub>	24	2.05	2.48	2023	4
16-50B	12Y 0A 2St	Si <sub>3</sub> N <sub>4</sub>	25.5	2.09	2.47	2023	4
16-52	CP85+8Y 0A	Si <sub>3</sub> N <sub>4</sub>	24	2.03	2.37	2023	4
16-54	10Y 0A 0St	Si <sub>3</sub> N <sub>4</sub>	16	1.77	2.13	2023	4
16-55	6Y 0A 0St	Si <sub>3</sub> N <sub>4</sub>	16***				

\*Y = Y<sub>2</sub>O<sub>3</sub>

A = Al<sub>2</sub>O<sub>3</sub>

St = stearic acid

\*\*Injection molded, all others are cold pressed.

\*\*\*Mill slipping.

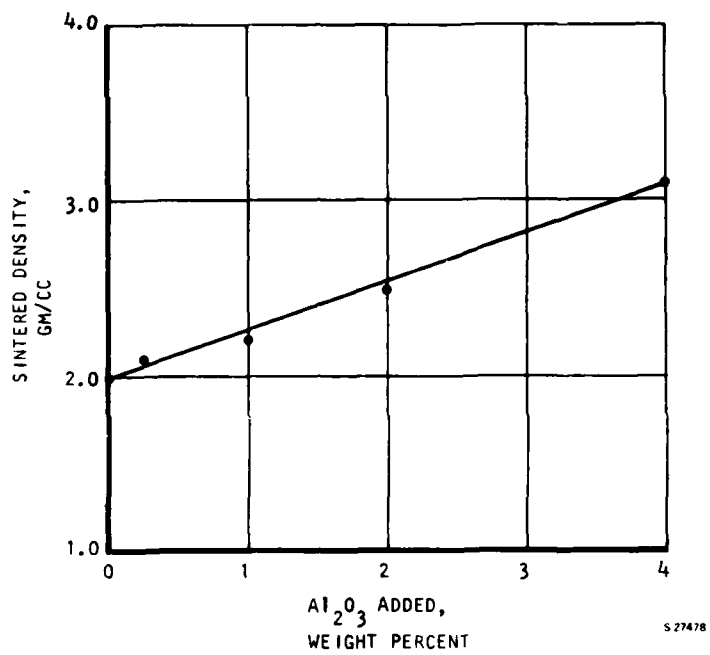


Figure 30. Sintered Density vs Weight/Percent of  $Al_2O_3$  (1998°K, 2 hr)

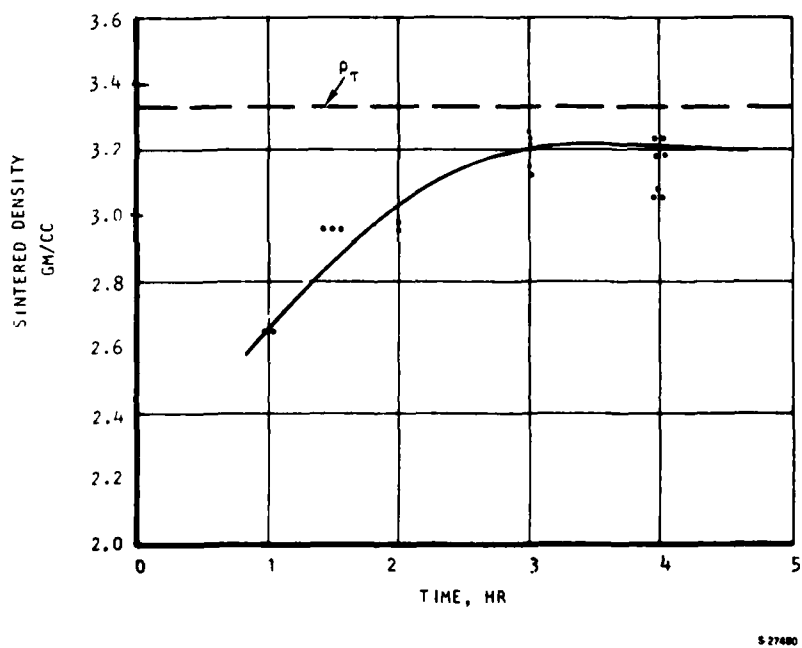


Figure 31. Sintered Density vs Sintering Time at 2023°K

and the other was sintered for 3 hr at the same temperature. The test specimens were as-sintered, injection molded bars 2.54 mm by 6.35 mm by 44.5 mm in size. The span was 19 mm and the crosshead speed was 0.5 mm/min. Three specimens were tested at room temperature and at 1588°K. The data of these tests are given in Table 15.

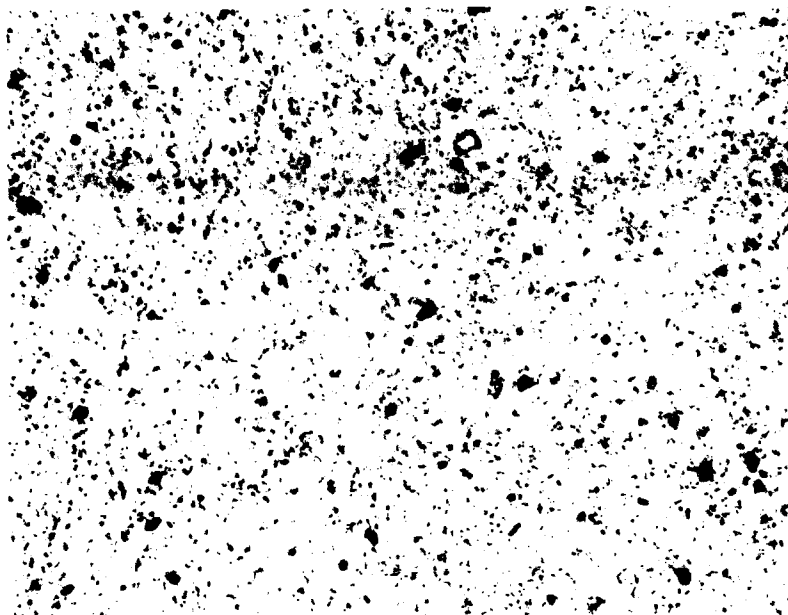
The polished cross-section microstructures of the sintered specimens are shown in Figure 32. The larger amount of free silicon (light areas) in the specimen sintered for longer time (3 hr) indicates a greater extent of decomposition at the sintering temperature in this specimen compared to the one sintered for 1.5 hr. (Therefore, the sintering time has to be optimized to get the best microstructure and density.) The elements lost in vaporization are mainly nitrogen and oxygen and some silicon. This gives rise to increased metallic inclusions.

Low magnification photos (Figure 33) of the polished specimens also show the structural (or compositional) difference between materials sintered for 1.5 and 3 hr. The 1.5-hr specimen is an off-white or cream color with few noticeable silicon inclusions. The 3-hr specimen has a banded structure with a dense, clear, outer layer surrounding a center with porosity and free silicon.

TABLE 15  
PRELIMINARY MODULUS OF RUPTURE (MOR) MEASUREMENTS

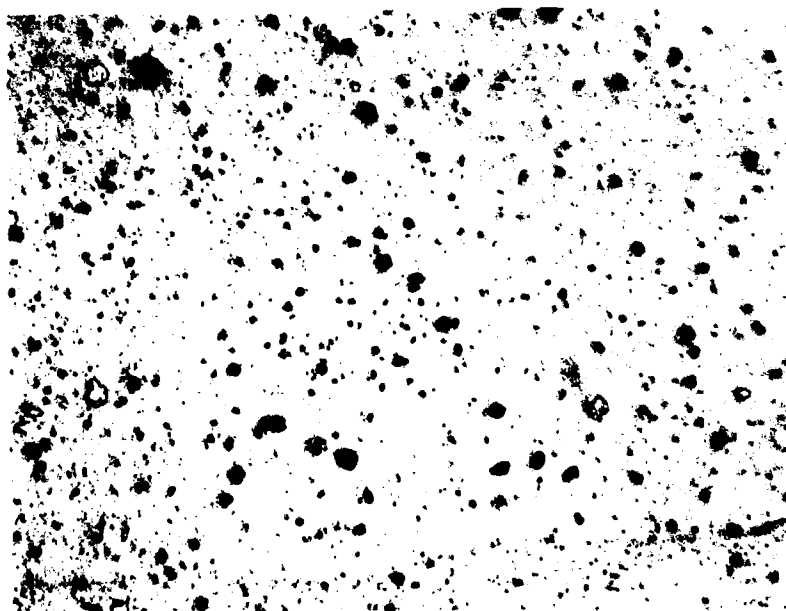
Specimen Type	Testing Temperature	4 Point MOR	
		MPa	ksi
Injection molded, as-sintered, 2023°K, 1.5 hr	Room temperature	427	62.0
		435	63.1
		442	64.1
	1588°K (1315°C)	124	18.0
		97.2	14.1
		165	24.0
Injection molded, as sintered, 2023°K, 3 hr	Room temperature	245	35.6
		247	35.8
		228	33.1
	1588°K (1315°C)	183	26.6
		168	24.4
		181	26.2

200X



SINTERED AT  
2023°K FOR 1.5 HR

200X



SINTERED AT 2023°K  
FOR 3 HR

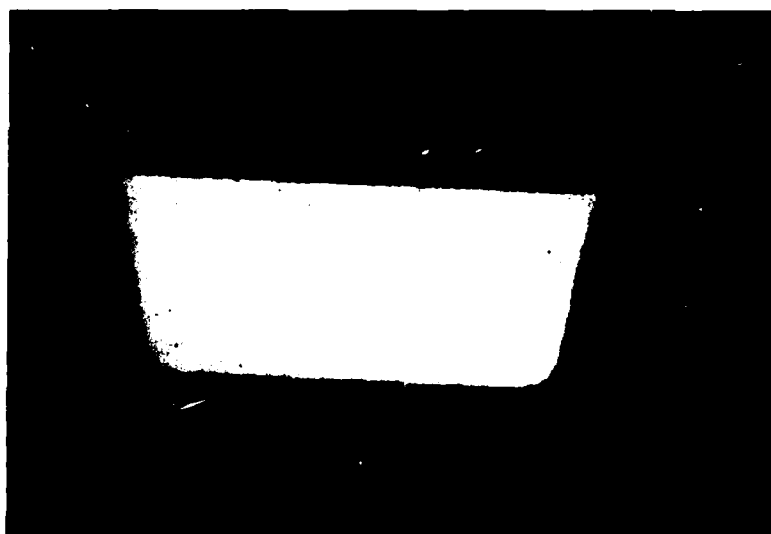
Figure 32. Microstructure of Si<sub>3</sub>N<sub>4</sub> Specimens

X10



SINTERED AT  
2023°K FOR 3 HR

X10



SINTERED AT  
2023°K FOR 1.5 HR

Figure 33. Polished Sections of 16-43 Material

A Philips-Norelco X-ray diffractometer employing monochromated  $\text{CuK}\alpha$  radiation was used at a scanning rate of 2 deg/min for XRD characterization of MOR specimens in the as-sintered condition and after 1588°F testing. For this purpose, the specimens were ground to fine powder. As-sintered silicon nitride (4 w/o  $\text{Al}_2\text{O}_3$  + 8 w/o  $\text{Y}_2\text{O}_3$ ) specimens showed only  $\beta\text{-Si}_3\text{N}_4$  solid solution as crystalline phase in the diffraction pattern (Figure 34). After MOR testing at 1588°K in air, the specimen showed a second crystalline phase (see Figure 35) which developed as a result of oxidation in air at the testing temperature. This phase has been identified as nitrogen apatite [ $\text{Y}_5(\text{SiO}_4)_3\text{N}$ ].

The weight loss of test specimens after binder removal and that of as-received GTE 502  $\text{Si}_3\text{N}_4$  powder heated for 1 hr at 1273°K in vacuum was determined. The results (Table 16) indicate that the injected vanes and test bars which had been through binder extraction at 578°K have 1-percent residual volatiles, apparently as a result of processing.

TABLE 16  
1273°K WEIGHT LOSS SUMMARY

Specimen Type	Weight Loss, Percent
Injected vane (after binder removal)	1.1
Injected test bars (after binder removal)	1.0
Dry-pressed disc	2.0
GTE 502 $\text{Si}_3\text{N}_4$ , as-received	0.1

The weight loss of injection molded parts as a function of time at 2023°K is shown in Figure 36. The data as plotted include the 1 percent loss at 1273°K due to remnant volatiles. Therefore, the weight loss that would bring about composition change in the specimen is restricted to a reasonable level of 1.5 percent for a sintering time of 1 hr.

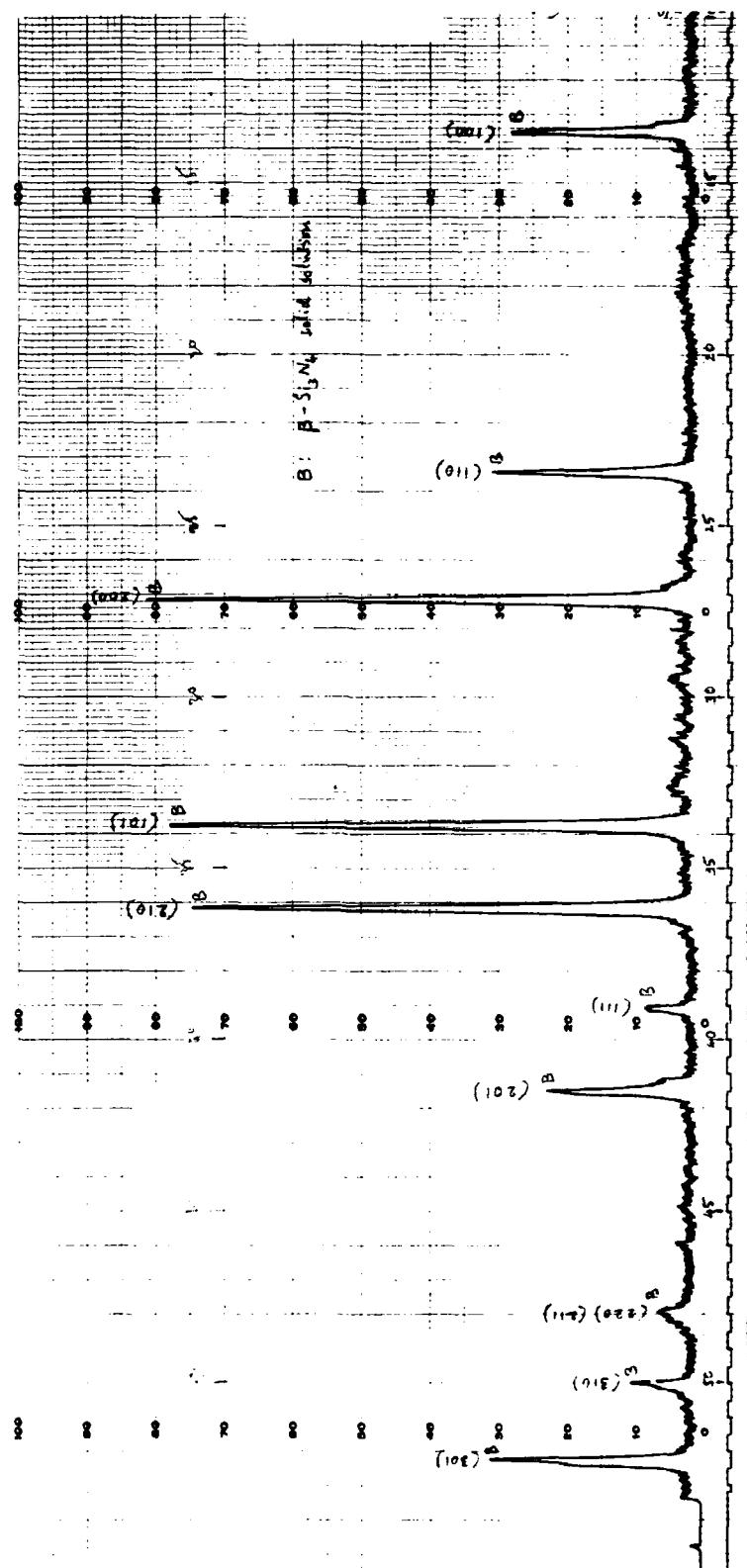


Figure 34. X-Ray Diffraction Pattern of As-Sintered MOR Specimen (Injection molded batch 16-43, CuK $\alpha$  radiation monochromated)

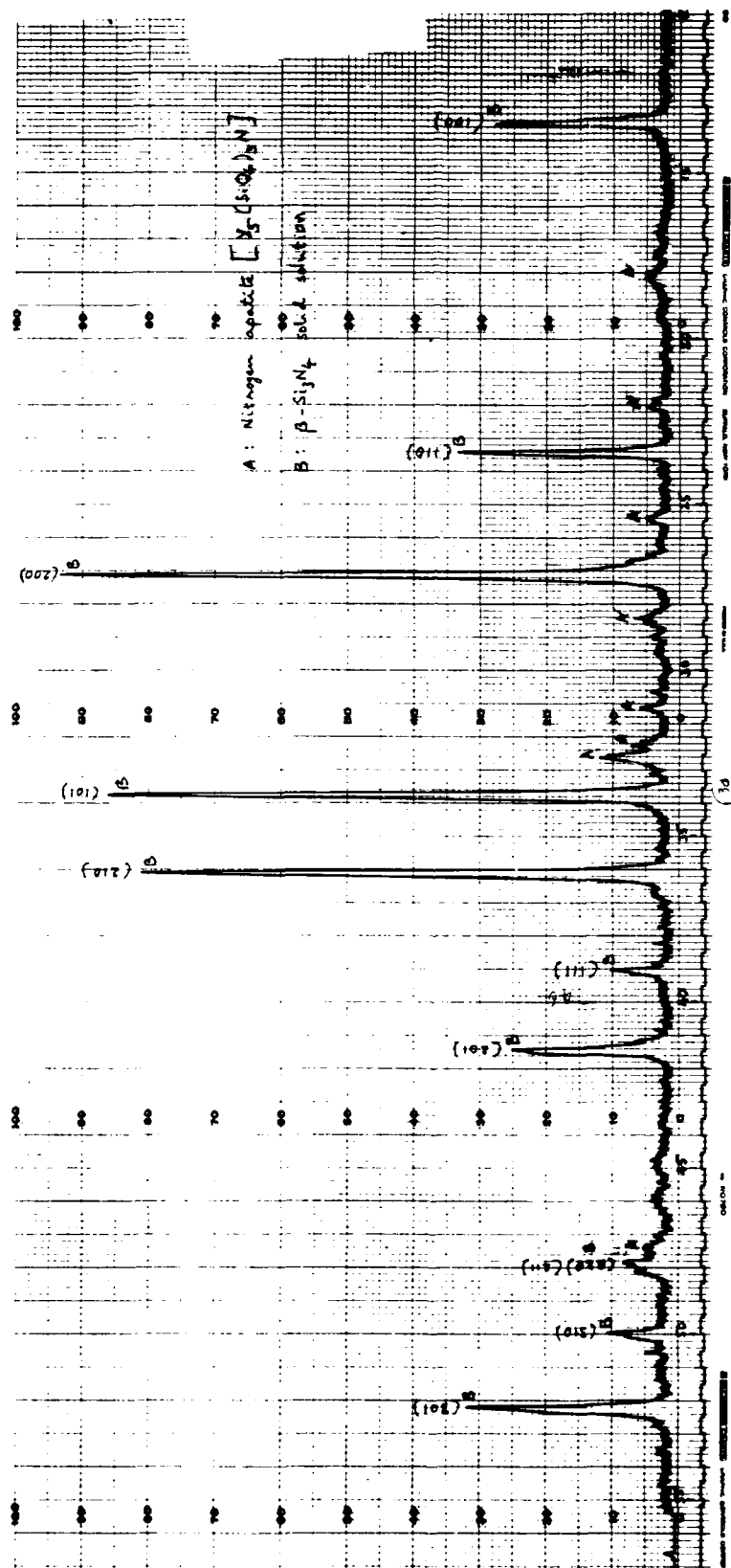
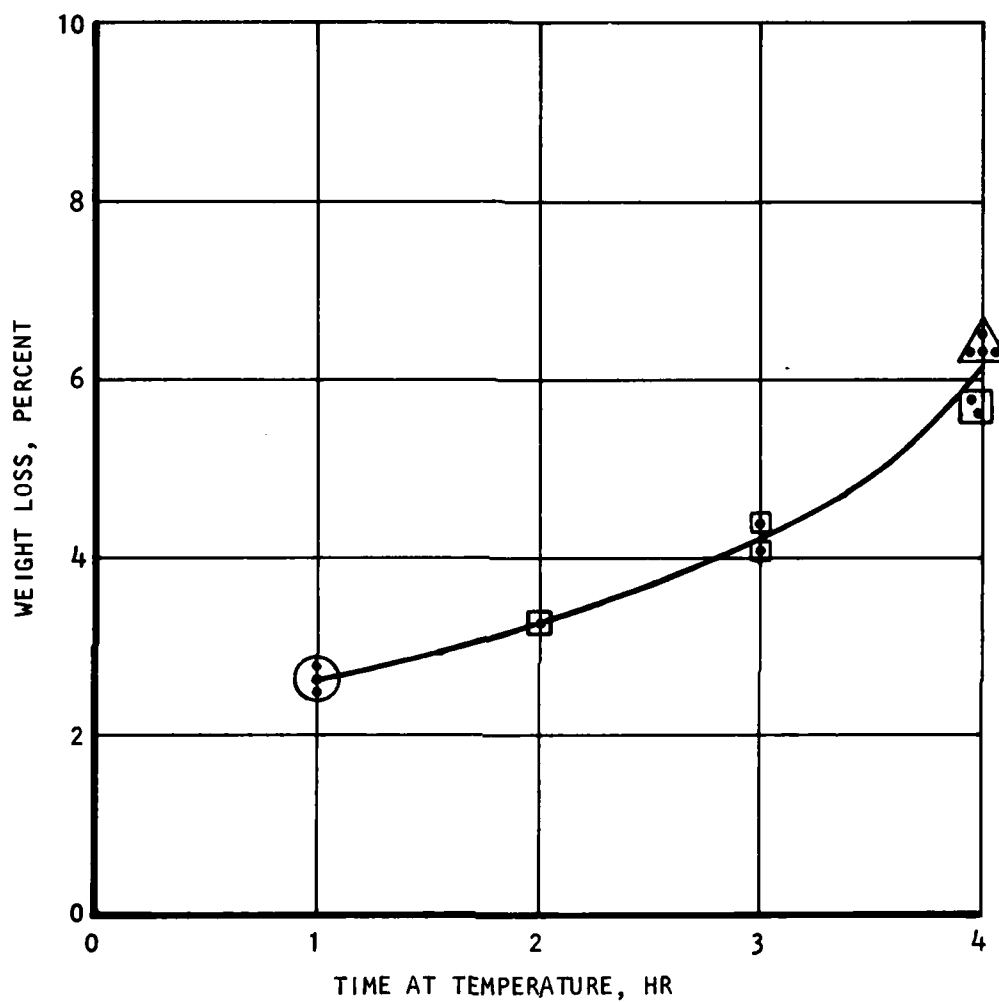


Figure 35. X-Ray Diffraction Pattern of MOR Specimen after 2400°K Test in Air (Injection molded batch 16-43, CuK $\alpha$  radiation monochromated)



INJECTION RUN	BATCH	COMMENTS
◻ = 04198	16-43	88 WT/% Si <sub>3</sub> N <sub>4</sub> , 8 WT/% Y <sub>2</sub> O <sub>3</sub> , 4 WT/% Al <sub>2</sub> O <sub>3</sub>
▲ = 04188	16-44	16-43 Si <sub>3</sub> N <sub>4</sub> MEDIA MILLED
● = 05168	16-43	16-44 STEEL MEDIA MILLED

S-27479

Figure 36. Weight Loss vs Time at 2023°K for Injection Molded Specimens

### 3.6.4 Sintering Response to Powder Preparation and Forming

Both cold-pressed discs and injection-molded bars were used to evaluate the sintering behavior of GTE 3512 powder and to compare it with the GTE 502-based composition 16-43. Data relating the sintering response to powder preparation and forming methods are listed in Table 17.

TABLE 17

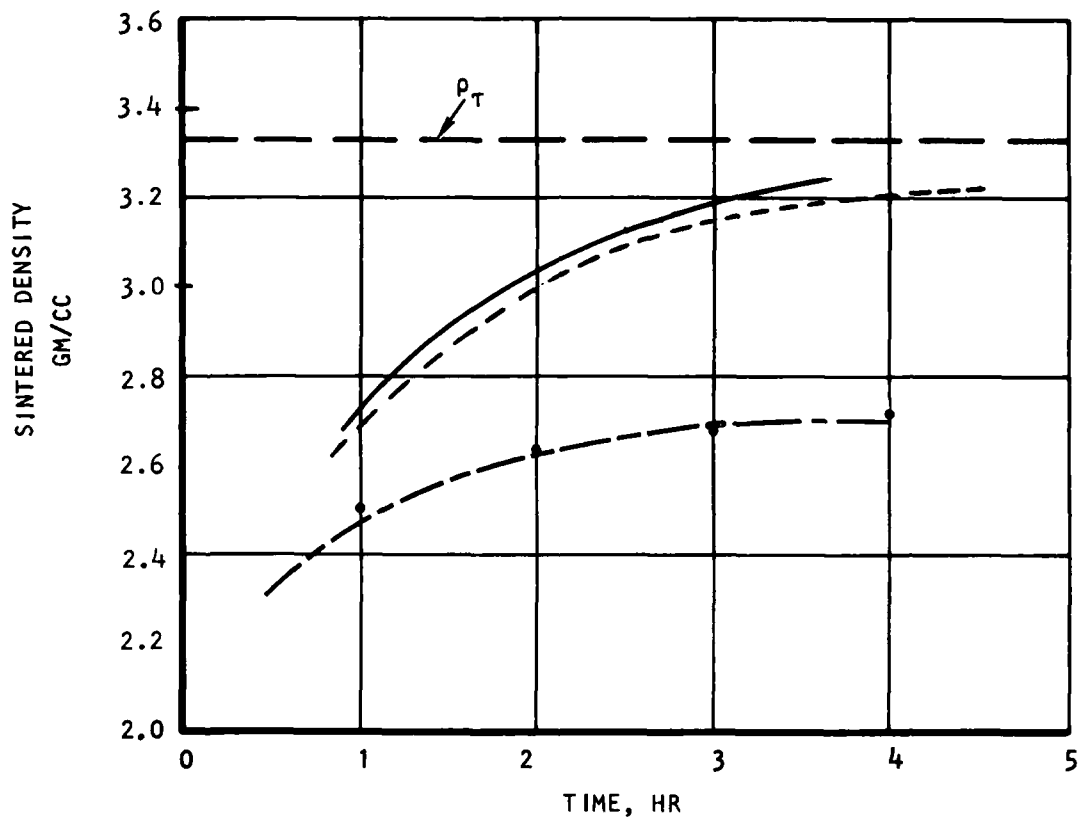
SINTERING RESPONSE OF COMPOSITION GTE 3512 TO POWDER PREPARATION

Material	Forming Method	Green Density, gm/cc	Sintered Density (2023°K, 1 hr), gm/cc
As-received	Cold press	1.77	2.03
22-hr dry ball milled	Cold press	2.21	2.45 to 2.55
As-received	Injection molded	2.15	2.44 to 2.54

Sintering times at 2023°K were varied from 1/2 to 4 hr. Densities from 2.31 to 2.66 gm/cc were obtained. These data are plotted in Figure 37 with that of 502 material fired for the same times.

Injection-molded samples of composition 16-43 (88 wt/% 502  $\text{Si}_3\text{N}_4$  + 8 wt/%  $\text{Y}_2\text{O}_3$  + 4 wt/%  $\text{Al}_2\text{O}_3$ ) were fired with each of the GTE 3512-based specimens. Sintered densities varied from 2.71 gm/cc at 2023°K for 1/2 hr to 3.16 gm/cc for 2 hr. This densification is essentially the same as previous batches with the same composition.

The sinterability of the two compositions is shown in Figure 37. It is readily apparent that the composition GTE 3512 material tested did not meet the criteria required to achieve 95 percent of theoretical density. Although both materials could be injection-molded into sound specimens, significantly higher sintered densities were achievable with composition 16-43. Therefore, composition 16-43 was selected for the balance of the program (sintering studies, property measurements, and AFML specimen preparation).



——— COMPOSITION 16-58 GTE 502 PLUS 8 WT/%  $Y_2O_3$  AND 4 WT/%  $Al_2O_3$   
 - - - - - COMPOSITION 16-43 GTE 502 PLUS 8 WT/%  $Y_2O_3$  AND 4 WT/%  $Al_2O_3$   
 - . - . - COMPOSITION 16-60 GTE 3512 (GTE PROPRIETARY DENSIFICATION AID)

S-27480 A

Figure 37. Sintered Density vs Sintering Time at 2023°K

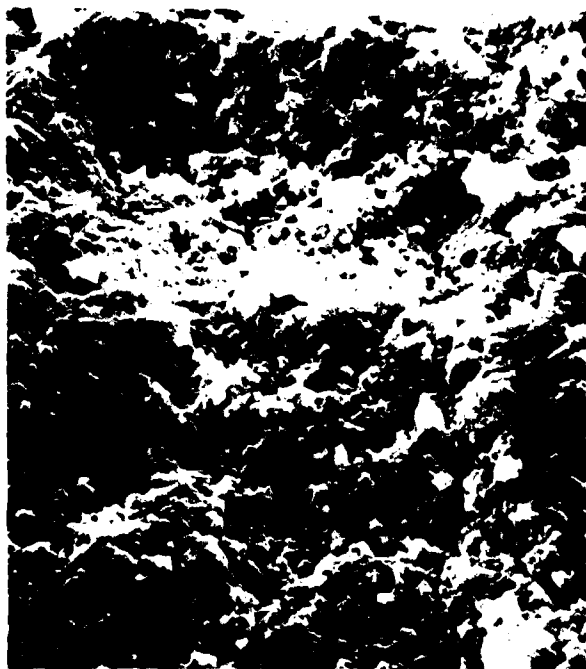
### 3.6.6 Sintering Parameter Study

A set of samples fabricated the same (up to the sintering step) as those shipped to AFML was used for a time-temperature sintering study. This experiment is summarized in Table 18.

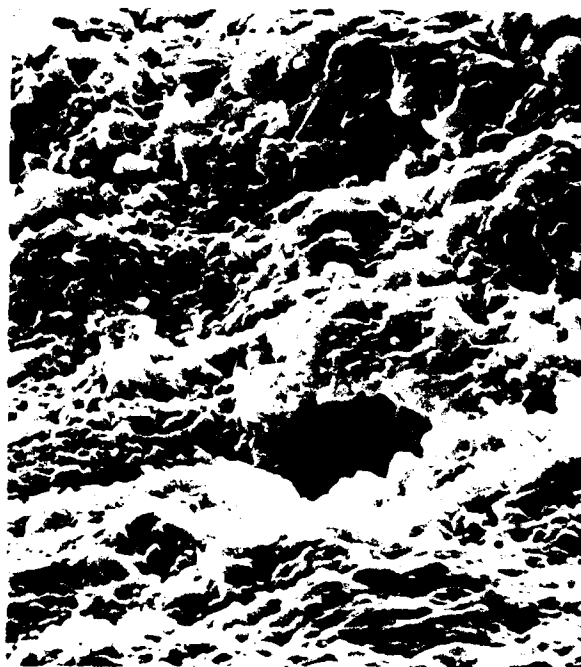
TABLE 18  
SINTERING PARAMETER STUDY

Material Tested: Batch 116-72 Composition: 88 weight/percent SN502, 8 weight/percent $Y_2O_3$ , 4 weight/percent $Al_2O_3$ Samples: Injection molded MOR test bars Number of samples: Four per sintering cycle Furnace atmosphere: Vac. to 1000°K, then to 0.21 Mpa $N_2$ Rate: 1 hr to 1000°K, 1 hr to 1923°K			
Part Numbers	Temp, °K	Time, hr	Avg Density, gm/cc
18-21	1923	1	2.80
37-41		3	2.89
33-36		5	3.11
5-8		1.5	2.93
9-13	1973	3	3.09
46-49		5	3.20
50-53		0.5	2.96
14-17		1	3.09
24-27	2023	3	3.21

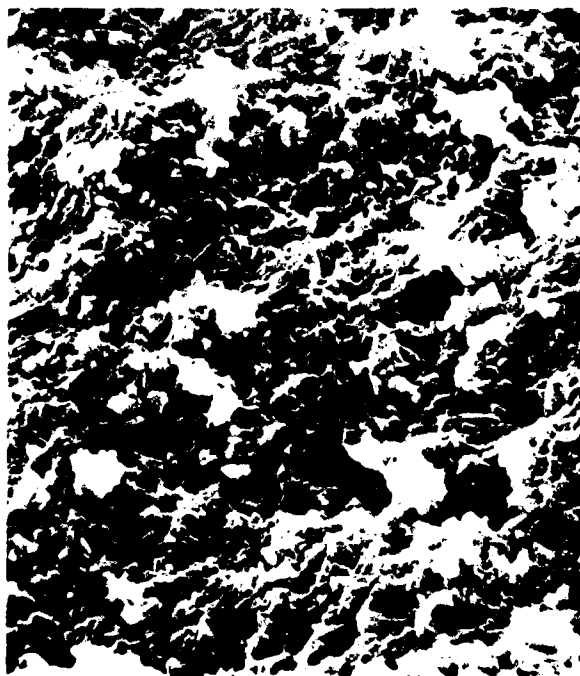
The modulus of rupture of each of the specimens was determined (refer to para. 3.7) and scanning electron microscopy was used to determine the material structures. Figure 38 shows the micrographs of the fracture surfaces and the nature of the structure development as a function of time and temperature.



1923°K, 1 HR



1923°K, 3 HR

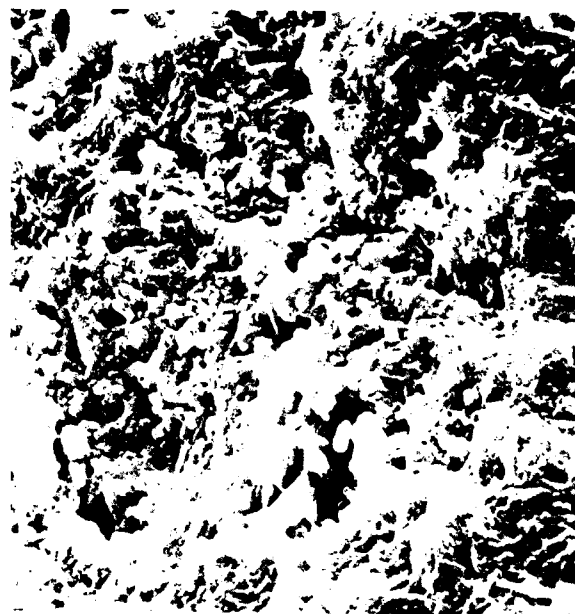


10 μm

Figure 38. Scanning Electron Micrographs of 88 wt/%  $\text{Si}_3\text{N}_4$ , 8 wt/%  $\text{Y}_2\text{O}_3$ , 4 wt/%  $\text{Al}_2\text{O}_3$  Sintered at Various Temperatures and Times

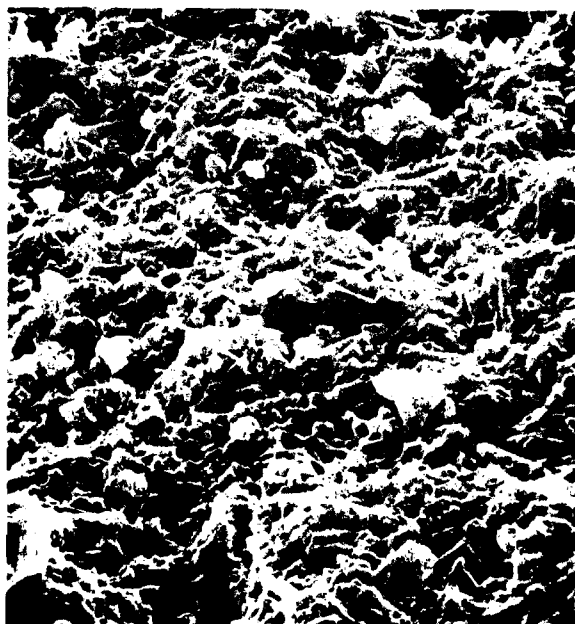


1973°K, 1.5 HR



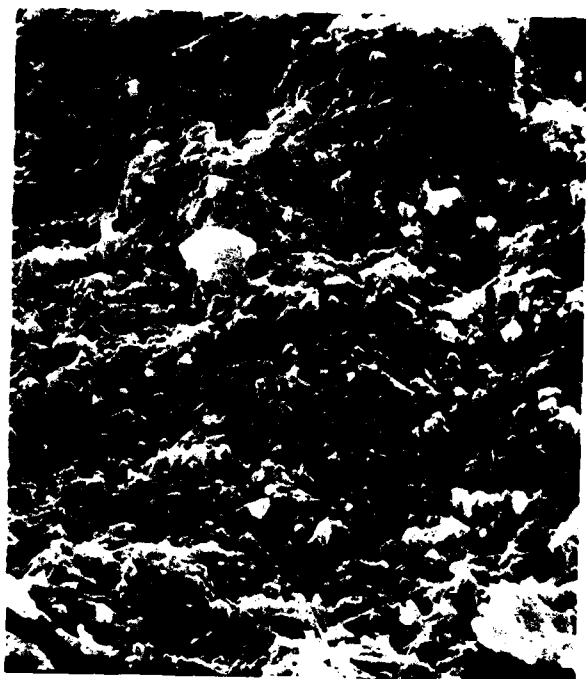
1973°K, 3 HR

10  $\mu$ m



1973°K, 5 HR

Figure 38. (Continued)



2023°K, 1 HR



2023°K, 3 HR

10  $\mu$ m

Figure 38. (Continued)

During the study of the fracture surfaces of the MOR specimens by SEM, it was noted that there was a significant amount of porosity related to the as-sintered specimen faces. Although not quantized, it did appear that the number and size of the pores was in direct relationship to the sintering time and temperature, with the most extensive pore development occurring in the 2023°K, 3-hr sintered material. An example of the structures noted is shown in Figure 39.

### 3.7 PROPERTIES MEASUREMENT

The room temperature strength of injection-molded specimens was determined by 4-point modulus of rupture. The self-aligning flexural strength fixture used is shown in Figure 40. The tests were made on unmachined test bars. The standard test bar configuration was 6.35 by 3.175 by 76.2 mm. A cross-head speed of 0.5 mm/min was used for all testing. The summary of the results for a strength vs sintering temperature/time experiment is given in Table 19. It is noteworthy that, contrary to usual experience, the maximum strengths do not occur with maximum density. This indicates an overfiring condition that was also apparent in the polished section and SEM observations. After approximately one hour at temperature, a porous surface layer resulting from decomposition becomes a very important characteristic of the sintering reaction. This is particularly significant in the case of the development of large surface pores as mentioned in para. 3.6.7. The presence of these pores, acting as surface defects on the tensile face of a modulus of rupture specimen, must adversely affect the strength results obtained. It was beyond the scope of this program to further investigate the nature and effect of this porosity. If there is a system of large pores related only to a thin surface layer, then machined specimens might produce a significant increase in strength results.

Definite large flaws were the cause of several of the specimen failures. The largest and most obvious defect noted is shown in Figure 41. This specimen, fired at 2023°K (1750°C) for 1 hour, failed at 334 MPa (48.5 ksi). A similarly processed specimen that had a strength of 420 MPa (61 ksi) is shown in Figure 42.

Additional test specimens made and shipped to AFML are described below:

- (a) Modulus of rupture--Rectangular bar-shaped, 50 samples, standard test bar configuration of 6.35 by 3.175 by 76.2 mm
- (b) Thermal diffusivity--Coin-shaped samples, 10. Samples were machined from plates formed in the ACC double torsion test injection molding specimen tooling; Configuration was 14.3 +0.13 mm diameter by 1.14 to 1.27 mm thick
- (c) Fracture toughness--Plate-shaped samples, 10, configuration was the same as item (a)

All specimens were X-rayed after sintering and the films were provided to AFML. Additional samples as required for ACC testing were fabricated the same as those shipped to AFML.

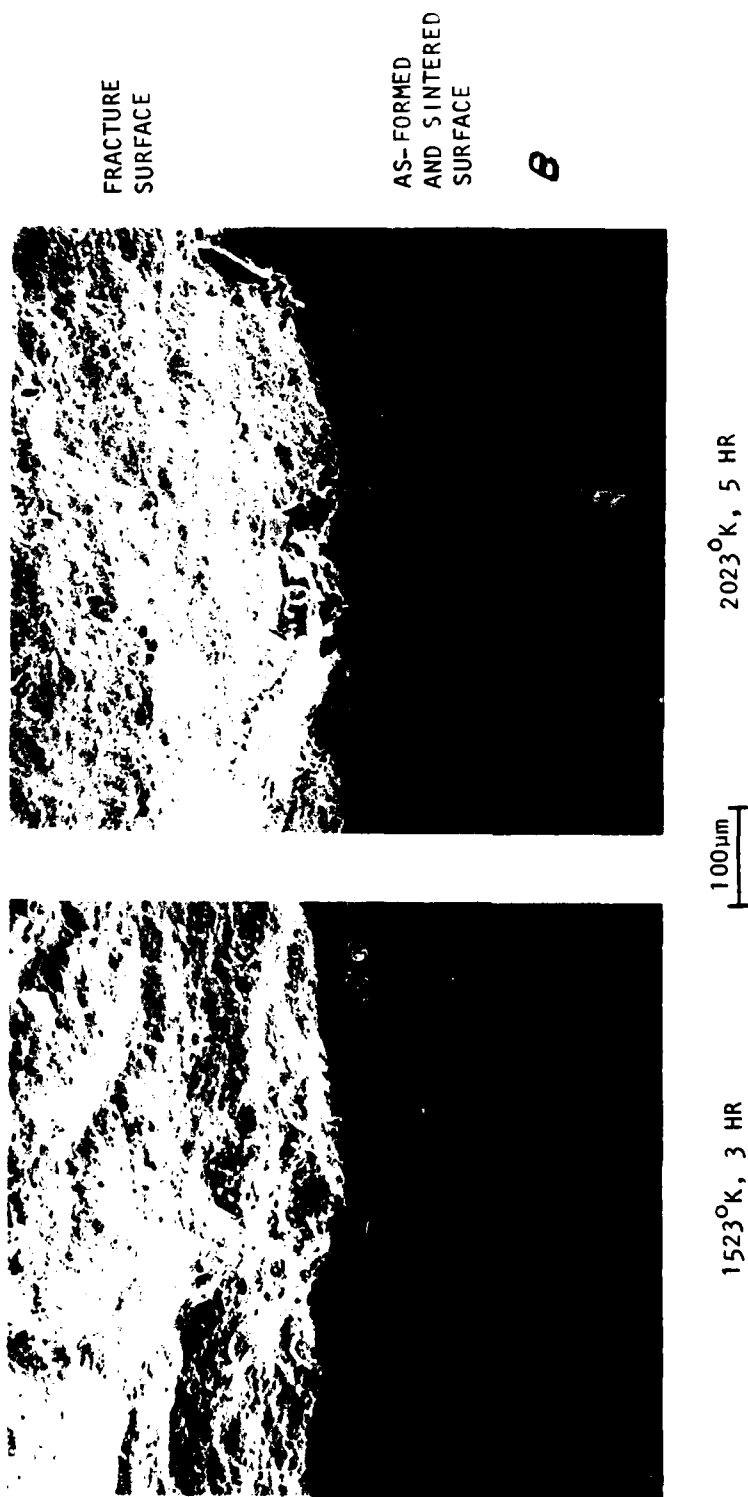


Figure 39. Scanning Electron Micrographs Showing Increased Surface Porosity with Sintering Time

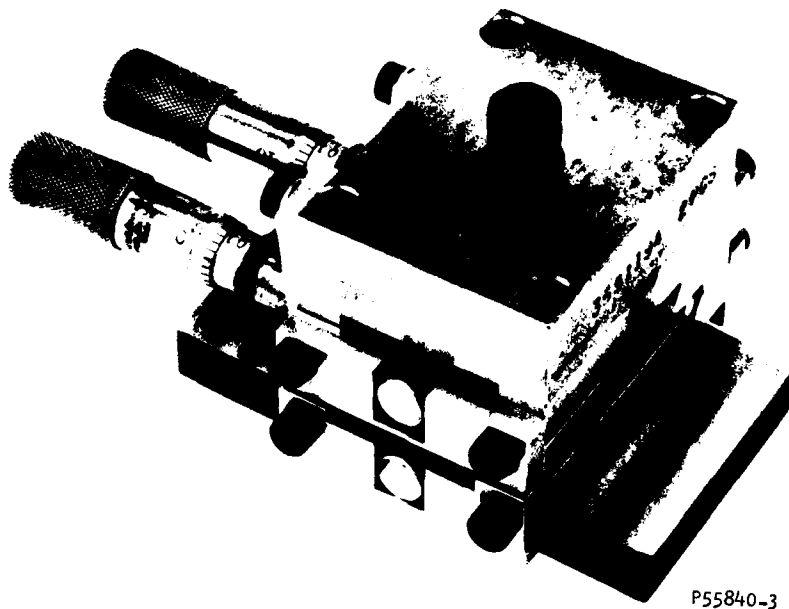


Figure 40. 4-Point Flexural Strength Fixture

TABLE 19  
MODULUS OF RUPTURE RESULTS

Sintering Temperature, °K, (°C)	Sintering Time, hr	4 Bar Averages MOR, MPa, (ksi)	Sintered Density, gm/cc
1923, (1650)	1	342, (49.6)	2.80
	3	354, (51.3)	2.89
	5	266, (38.6)	3.11
1973, (1700)	1		
	1.5	366, (53.1)	2.93
	3	373, (54.1)	3.09
	5	214, (31.1)	3.21
2023, (1750)	1/2	-	2.96
	1	402, (58.3)	3.09
	3	352, (51.1)	3.21

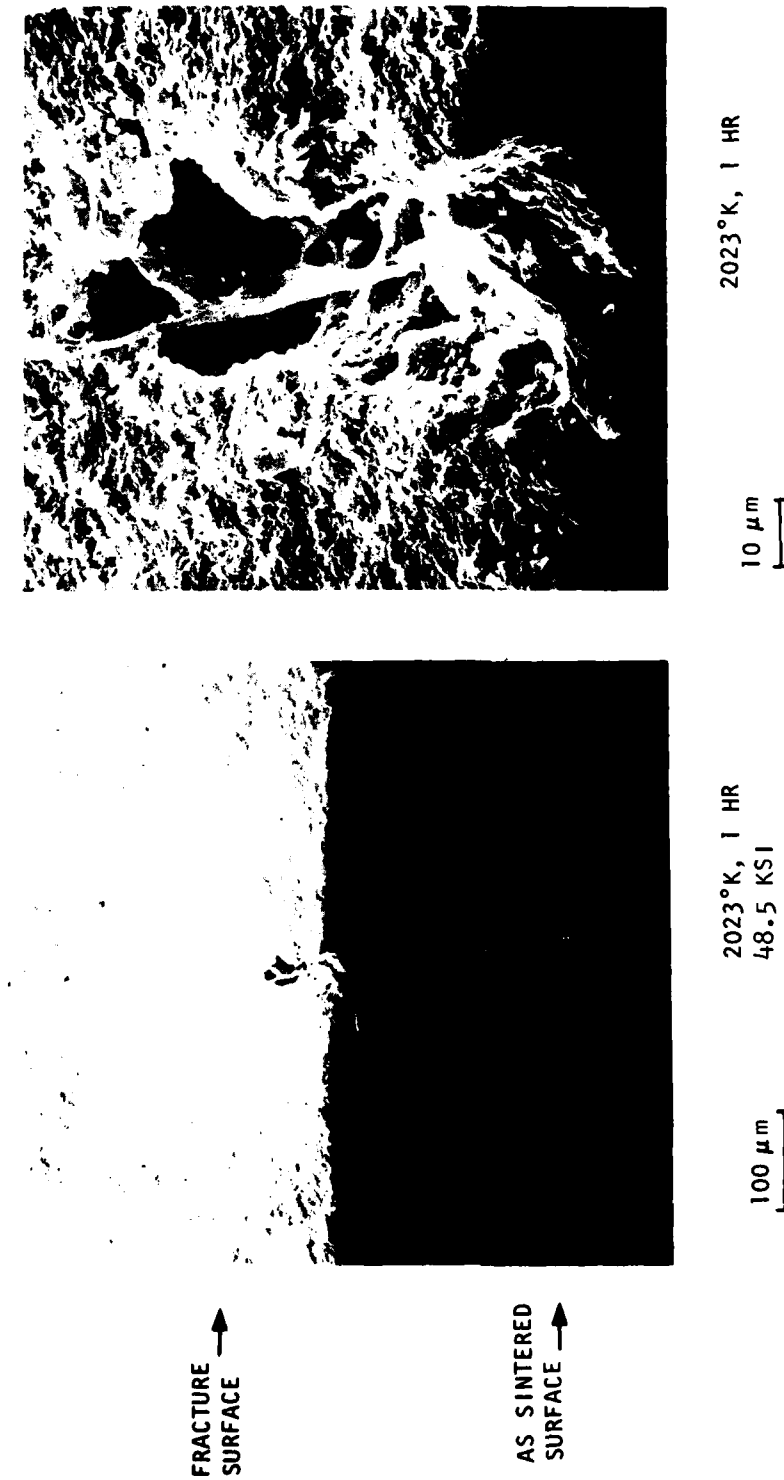


Figure 41. Large Defect on Tensile Surface of Sintered MOR Specimen

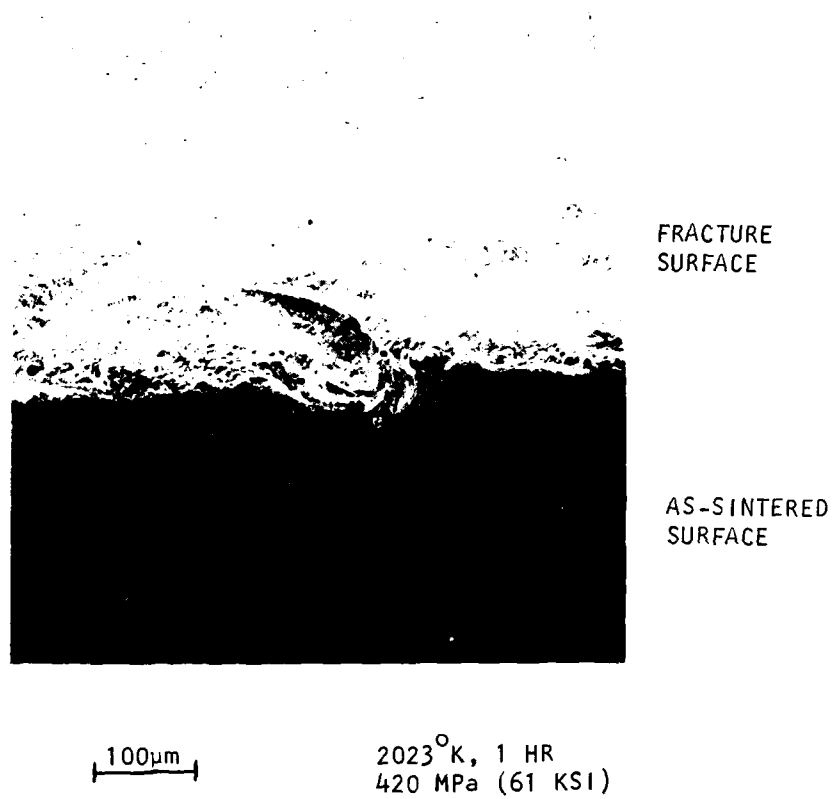


Figure 42. Apparent Fracture Origin in 61 KSI MOR Test Specimen

### 3.8 PROCESS DESCRIPTION

The process and materials described in Table 20 resulted from the many experiments performed on this program and were used to fabricate the test specimens submitted to AFML.

TABLE 20  
TEST SPECIMEN PROCESS AND MATERIALS

Starting Materials:				
Silicon nitride: Type SN502 - GTE Sylvania, Towanda, Pa.				
Yttrium oxide: Type 5600 - Molycorp, Louviers, Colo.				
Aluminum oxide: Linde-A - Union Carbide				
Stearic acid: MCB, practical grade				
Binder/lubricant: LN-27-266-2, J. F. McCaughin Co., Rosemead, Calif.				
Process Details:				
Operation	Controller Process Variables	Recommended Limits (1)	Recommended Control Techniques	Process Equipment Description
Material batching 616 gms $\text{Si}_3\text{N}_4$ 56 gms $\text{Y}_2\text{O}_3$ 28 gms $\text{Al}_2\text{O}_3$ 14 gms stearic acid	Weights	$\pm 0.1$ GM $\pm 0.01$ $\pm 0.01$ $\pm 0.01$	-	Sartorius 3716 Balance
Milling	Time: 24 hr Percent critical speed ( $N_c$ ): 60 percent Media to charge: 2:1	$\pm 1$ $\pm 2$	Pressed green density Surface area Particle size distribution	20 cm ID rubber lined mill 17 x 17 mm cylindrical $\text{Si}_3\text{N}_4$ media
Blending 1200 gms milled powder 184 gms LN27-266-2	Temp: 394°K Time: 2 hr	3°K $\pm 5$ MIN		Sigma Blade mixer Model 50B P.O. Abbe Co., Little Falls, N.J.
Pelletizing	Output particle size	<8 mesh		Model 46 pelletizer, Polymer Mach. Co., Berlin, Conn.
Injection molding	Injection speed: 5 Injection press: 12.4 MPa Injection hold time: 5 sec Injection temp.'s: Feed zone: 344°K Plasticizing zone: 350°K Nozzle: 350°K Mold temp: 500°K Mold clamp time: 36 sec	4 to 5 11-12.4 MPa (2) $\pm 3^\circ\text{K}$ $\pm 3^\circ\text{K}$ $\pm 3^\circ\text{K}$ $\pm 5^\circ\text{K}$ 10 to 36 sec	Radiography 10-20X optical	221E/150 Arburg Allrounder, Polymer Mach. Co., Berlin, Conn.
Binder extraction	Temp: rm to 578°K Time: 24 hr Atmos: Vacuum	$\pm 2^\circ\text{K}$ $\pm 1$ hr <1000um Hg	CR/Al thermo-couple T/C qage	Vacuum oven (see Sec. 3.5)
Sintering	Temp.-Time: 1 hr to 1000°K, 1 hr to 1923°K $\pm 10^\circ\text{K}$ 1923°K, 3 hr Atmos: Vac. to 1000°K, 0.21 Mpa $\text{N}_2$ balance of cycle		Optical pyrometer W-Re Thermo-couple	Vacuum/pressure Sintering furnace (see Sec. 3.6)

NOTES: (1) Limits within which satisfactory results were obtained on this program.  
(2) Limit not measured.

## SECTION IV

### CONCLUSIONS

This program met its goal to demonstrate that injection molding is a viable process for the fabrication of complex shapes using a commercially available  $\text{Si}_3\text{N}_4$  powder with suitable densification aids. A comparison of parts made by uniaxially cold pressing vs injection molding showed that the injection process was capable of producing parts that were equivalent or in some cases superior in their sinterability.

Rather extensive pore development, both internal and surface, occurs at the sintering temperatures used ( $1923^\circ$  to  $2023^\circ\text{K}$ ) even with 2 atmospheres nitrogen overpressurization.

The tested GTE 3512  $\text{Si}_3\text{N}_4$  powder, which reportedly is a SN502  $\text{Si}_3\text{N}_4$  with the sintering aid added by the manufacturer, was not as sinterable as a composition consisting of 88 wt/% SN502  $\text{Si}_3\text{N}_4$ , 8 wt/%  $\text{Y}_2\text{O}_3$ , and 4 wt/%  $\text{Al}_2\text{O}_3$ , which was sintered to greater than 95 percent of theoretical density.

Dry ball milling for 16 hours is an effective method of comminution of the acicular crystal present in the SN502 type of silicon nitride powder.

The SN502 powder milled with noncontaminating  $\text{Si}_3\text{N}_4$  grinding media would not sinter to high density with the use of up to 8 wt/%  $\text{Y}_2\text{O}_3$ ; however, the addition of  $\text{Al}_2\text{O}_3$  through the  $\text{Al}_2\text{O}_3$  milling media or by the controlled addition of  $\text{Al}_2\text{O}_3$  powder did result in a composition capable of being sintered to a density greater than 95 percent of theoretical.

## SECTION V

### RECOMMENDATIONS

The preliminary high temperature results obtained suggest the need for additional material studies to optimize the Y-Si-Al-O-N system. Although this was a fabrication process study rather than a materials optimization program, the density and strength results obtained with the Y-Si-Al-O-N system were encouraging. Optimization of this material, particularly with respect to sintering and the reduction of strength limiting defects such as surface porosity, is expected to significantly increase the modulus of rupture over the 442 MPa room temperature and 247 MPa elevated (1580°K) temperature results obtained.

The surface porosity noted on the modulus of rupture specimens suggests the need for compositions sinterable at lower temperatures, or the use of higher nitrogen overpressure during sintering. The effect of removal of the porous surface by machining should be determined so that this possible defect might be eliminated from the evaluation of the inherent strength of the composition of interest.

The injection molding fabrication technique should be applied to other sintering systems as they become available since this program demonstrated that injection molded parts can be sintered to the same density as cold pressed parts.

## REFERENCES

1. Naik, I. K. and T. Y. Tien, "Subsolidus Phase Relationships in Part of the System Si, Al, Y/N, O," presented at the 80th Annual Meeting of the American Ceramic Society, Detroit, Mich., May 1978 (Basic Science Division, Paper 147-B-78), to be published in J. Am. Ceram. Soc.
2. Rowcliffe, D. J. and P. J. Jorgensen, "Development of a Low-Cost Process for the Fabrication of Fully Dense Silicon Nitride High-Temperature Gas Turbine Components," Final Report for NSF Grant No. AER 75-14896, SRI, Menlo Park, Calif., Dec. 1, 1977.
3. Jack, K. H., "Review--Sialons and Related Nitrogen Ceramics," J. of Materials Science, Vol. 11, p. 1135, 1976.
4. Lange, F.F., S. C. Singhal and R. C. Kuznicki, "Phase Relations and Stability Studies in the  $\text{Si}_3\text{N}_4$ - $\text{SiO}_2$ - $\text{Y}_2\text{O}_3$  Pseudoternary System," J. Amer. Ceram. Soc., 60 [5-6], pp. 249-252, 1977.
5. Naik, I. K., L. J. Gauckler and T. Y. Tien, "Solid-Liquid Equilibria in the System  $\text{Si}_3\text{N}_4$ - $\text{AlN}$ - $\text{SiO}_2$ - $\text{Al}_2\text{O}_3$ ," ibid, 61 [7-8], pp. 332-35, 1978.
6. Phase Diagrams for Ceramists, Editors: E. M. Levin, C. R. Robbins, and H. F. McMurdie, Figure 2586, p. 165, American Ceramic Society, Columbus, Ohio, 1969.
7. Mencik, Z. and M. A. Short, "Quantitative Analysis of Synthetic Silicon Nitride by X-Ray Diffraction: An Improved Procedure," Technical Report SR-72-98, Ford Motor Co. Scientific Research Staff, Dearborn, Mich., Sept. 5, 1972.
8. Gazzara, C. P. and D. R. Messier, "Determination of Phase Content of  $\text{Si}_3\text{N}_4$  by X-Ray Diffraction Analysis," Ceramic Bulletin Vol. 56, p. 777, 1977; and AMMRC Report TR 75-4, February 1975.